Effects of MgO on

Self-healing Properties of Cements

by

Marjan Fayaz Torshizi (T)

Fourth-year undergraduate project
in Group D, 2013/2014

I hereby declare that, except where specifically indicated, the work submitted herein is my own original work.

Date: Signature:

Technical Abstract

The production of Portland cement (PC) through calcination at high temperatures leads to a significant amount of CO_2 emissions annually (5-7% in 2009). Furthermore the formation of cracks in concrete due to its low tensile strength has lead to huge costs for the repair and maintenance of concrete structures. Postponing the need for maintenance will lead to a reduction in the costs incurred. Ensuring a better structural integrity, through prevention of crack development will help achieve this. One way of doing so is by adapting self-healing technology in the making of concrete.

PC exhibits intrinsic self-healing properties up to a certain extent upon hydration. Several mechanisms for the natural self-healing ability of cement pastes have been identified such as swelling of the hydrated cement, further hydration of un-hydrated cement particles, precipitation of calcium carbonate and the blockage of crack faces. There are two types of self-healing: autonomic self-healing has entailed the use of microcapsules and hollow fibres containing healing agents, which are released automatically upon the formation of cracks; Autogenic self-healing of cementitious materials, on the other hand involves using the natural self-healing ability of cement blends or enhancing this ability through the incorporation of mineral admixtures that would normally be present in the composition of cement pastes, though in different proportions.

This report focuses on the autogenic self-healing ability of cement pastes. Of particular interest is the effect of magnesium oxide and slag on cement properties. Existing work includes the use of expansive mineral additives such as calcium sulfo-aluminate-based ones, bentonite clay, quicklime and magnesium oxide. Other mineral additives such as ground granulated blast-furnace slag and fly ash have also been used to enhance the durability and strength of cement pastes. Magnesium oxide has been found to offer several advantages over the conventional mineral additives such as the ability to control its expansive properties and higher stability under high temperatures. It also offers an enhanced ability to accommodate impurities such as industrial by-products. The replacement of PC in a cement paste with GGBS (ground granulated blast-furnace slag) has proven to reduce CO_2 emissions compared to 100% PC paste. It has been proven to yield a higher proportion of strength-enhancing calcium silicate hydrates than in normal PC pastes as well as a lower heat of hydration (which could possibly eliminate the problems associated with thermal shrinkage that lead to crack formation). The incorporation of MgO in GGBS-PC pastes has not been widely researched or studied before.

For this report two types of reactive magnesium oxide (N50 and 92/200, N50 being much more reactive than 92/200) were added to mixes containing PC only and mixes containing PC and GGBS in equal amounts. Control pastes including 100% PC and 50:50 GGBS-PC were also made for

comparison purposes. 3%,5% and 7% MgO content were tested for each type of MgO. 6 prisms and 9 cubes were produced per mix. Three prisms from each mix were cracked in a controlled manner on day 1 using three-point bending and left in curing tanks for 14 days to test for crack healing and mechanical strength recovery on day 14. The three un-cracked prisms were also cured for 14 days and then tested to compare the effect of ageing on mechanical strength. The cracks were also monitored using digital microscopic imaging. Cubes were tested in batches of 3 (on day 1, 3 and 14) for compressive strength development. The water to binder ratio for the mixes was determined using standard consistency tests and a fixed amount of superplasticiser was added to enhance the workability of the mixes. Furthermore hydration products of 100% PC, 5% MgO N50-PC and 5% MgO 92/200-PC were analysed using XRD.

It was concluded that the addition of both types of MgO results in a reduction in compressive strength of the mixes compared to the 100% PC mix. Of all MgO-PC mixes, 3% MgO N50 and 5% MgO 92/200 resulted in the highest compressive strengths after 14 days, however still much lower than 100% PC mix. The development of MgO 92/200 was faster than PC for the first 3 days, after which no significant development was observed. The strength development of MgO N50 however seemed to continue consistently, with a slight deceleration after day 3. For mixes containing MgO 92/200 and GGBS-PC, an increase in compressive strength was observed for all 3 contents from day 3-14, unlike MgO-PC mixes, which suggests that the presence of GGBS has helped improve the strength. The addition of GGBS alone to the PC mix resulted in an increased rate of development from day 3-14 compared to PC, though it still resulted in a lower compressive strength. GGBS is known for its early-age low and long-term high compressive strength.

Flexural strength recovery and crack width recovery were found to be dependent on one another: The smaller the cracks on day 1, the higher the percentage recovery of the mix on day 14 when re-cracked. The addition of MgO in general had increased the self-healing ability of the mixes and high crystal precipitation was observed when MgO 92/200 was used in 100% PC and GGBS-PC mixes, which could be due to the latent hydration of this type of MgO compared to N50. The mixes containing MgO 92/200 and GGBS yielded the highest flexural strengths on day 1. For 14-day cured samples, the addition of MgO 92/200 to the PC mixes significantly improved the flexural strength, with a 7% content yielding the highest strength. The addition of MgO N50 did not significantly improve the flexural strength on day-14 compared to 100% PC mix. The same trend was observed for samples containing GGBS and PC: The addition of 7% MgO 92/200 yielded the highest strength. The results from XRD analysis suggested that further testing was needed to identify the products formed in the presence of MgO. Finally, a risk assessment evaluation was also performed followed by possible future work.

Table of Contents

Acknowledgements

The author of this report would like to thank:

- Dr Al-Tabbaa for her on-going guidance and supervision throughout the year
- Mr Qureshi and Mr Abdollahzadeh for their assistance and advice, and most importantly teaching the experiment methods needed to perform the tests and helping with the analysis of results
- Mr Knight for his assistance in the geotechnical laboratory
- Family and friends for their continuing support throughout the year

1 Introduction

1.1 Motivation

Concrete is the most widely used material in the world. Approximately 3.4 billion tonnes of cement was produced in 2011 globally (USGS, 2012). This amount of cement production resulted in 2 billion tonnes of CO_2 emissions from the energy intensive processes of calcination and fuel usage (Global CCS Institute, 2013). In 2009, the cement industry contributed to 5-7% of anthropogenic global CO_2 emissions (IEA, 2009); therefore increasing the efficiency in concrete production can help reduce CO_2 emissions significantly.

Furthermore, due to a lack of quality in cement-based infrastructures worldwide, many countries have incurred unnecessary high costs to reconstruct, maintain and repair structures. In the U.S, $18-21 billion is needed annually to repair deteriorating structures and in 2006 it was estimated that a five-year plan worth $2.2 trillion is needed to maintain and repair structures (Vision 2020, 2006). Similarly in the UK, 50% of the construction budget is spent on repair and maintenance of structures, with 30% spent on concrete ones, of which 15-40% is allocated to hidden costs, which include traffic delays due to maintenance (Heriot-Watt University , 2012).

Given the growing environmental and economical concerns, the phenomenon of self-healing has been given a lot of attention recently. The adaptation of this technology could result in the postponement of repairs and a reduction in costs incurred. Self-healing concrete can act to close cracks that have propagated in structures using healing agents.

The process of self-healing has been classified into two groups by RILEM (The International Union of Laboratories and Experts in Construction Materials, Systems and Structures): autogenic and autonomic. According to this classification, autogenic self-healing occurs when materials used in the concrete structure are those that would otherwise be present when the structure is not designed for self-healing.

Autonomic self-healing has been defined as a process where the materials used are only present to activate the self-healing process. These materials are known as healing agents. This type of self-healing was first introduced by Dry where hollow porous fibres were designed to be filled with healing agents to be released upon the degradation of the fibre coating (Dry, 1992). Apart from the use of hollow fibres, other techniques such as microencapsulation of healing agents (Yang, Hollar, He, & Shi, 2011), designing a smart concrete for the application of selective heating around cracks (Nishiwaki, Jang, & Mihashi, 2006) and the incorporation of bacteria (Ghosh, 2009) have been explored.

There are different definitions of autonomic and autogenic self-healing according to different institutions worldwide. In this report it is assumed that changing the mix composition of concrete to enhance its performance by adding mineral additives and expansive agents falls into the autogenic self-healing category. MgO, a mineral additive used to compensate for the shrinkage of concrete upon setting, has the potential to enhance the autogenic self-healing properties of concrete. Currently the most widely used type of cement is Portland cement, which already has a trace of magnesium oxide in its composition. The production of PC is energy intensive and using a cement blend of PC and ground granulated blast-furnace slag (GGBS) has proven to reduce the environmental impacts as well as to enhance the material properties of the concrete produced. The focus of this project will therefore be evaluating the effect of MgO on PC pastes, as well as on PC-GGBS mixtures.

1.2 Aims & Objectives

The aim of this project is to investigate the effect of MgO as an expansive mineral additive on enhancing the autogenic self-healing ability of mixtures made from both traditional cement and a blend of GGBS and PC. The aims of this project are therefore:

- To assess the natural self-healing ability of PC without the use of mineral additives
- To investigate the effect of MgO type and content on self-healing of OPC pastes
- To assess the effect of GGBS on self-healing abilities of PC and MgO samples
- To compare the mechanical properties of MgO samples to PC and 50:50 GGBS-OPC blends

2 Literature Review

2.1 Introduction

Producing cementitious materials with enhanced performance in the first place results in a reduction in maintenance and repair costs in the future. Autogenic and autonomic self-healing techniques have offered promising solutions to overcoming the economical and environmental constraints associated with concrete production. In this chapter, a review of current developments in the field of self-healing will be presented, focusing on the advancements in autogenic self-healing.

2.2 Cracking in Cementitious Materials

Concrete is very strong in compression and typically has a compressive strength of 20-60 MPa, which can change to as high as 200 MPa by reducing its water/cement ratio. The low tensile strength of concrete however causes the formation of cracks. Crack formation can be due to shrinkage, thermal expansion, thawing, creep and other factors. Although the cracks formed could be very small, they lead to a reduction in toughness and durability and can eventually lead to failure of structures. One of the main sources of tensile stresses formed in cementitious structures is mechanical loading, which leads to visible crack formation, while other factors such as shrinkage and damaging chemical reactions can also lead to crack formation inside the structure. Early-age cracking of concrete occurs due to thermal and chemical shrinkage and moisture variation during the hardening of pastes. The combination of cement with water yields an exothermic reaction. The heat released is often termed the heat of hydration, which often leads to a temperature gradient between the interior and the exterior of the structure (particularly in thicker cross-sections of structures). The addition of mineral admixtures can help enhance the autogenic self-healing ability of cement pastes.

2.3 Autogenic Self-healing

2.3.1 Natural Self-healing of PC

Portland cement is the most commonly used hydraulic cement in the world. It is made from finely ground Portland cement clinker. The clinker is mostly made of calcium oxide, silica, aluminium oxide and iron oxide. These oxides form the four major compounds of the clinker. The proportion of these major compounds to produce ordinary Portland cement (Type I Portland Cement, OPC) is summarised in table 2.1 (Van Oss, 2002).

Chemical Formula	Description	%	Mineral Function
Ca_3SiO_5	Tricalcium silicate ('alite')	50-65	Hydrates quickly and imparts early strength and set
Ca_2SiO_4	Dicalcium silicate ('belite')	10-30	Hydrates slowly and imparts long term strength
$Ca_3Al_2O_6$	Tricalcium aluminate	6-14	Hydrates almost instantaneously and very exothermically. Contributes to early strength and set
$Ca_4Al_2Fe_2O_{10}$	Tetracalcium aluminoferrite	7-10	Hydrates quickly. Acts as a flux in clinker manufacture. Imparts gray color

Table 2.1- Major Compounds of OPC (Van Oss, 2002)

The raw materials are fed into a kiln and heated at 1400° C for the clinker to form. After cooling, 5% gypsum is often added to prevent early setting of cement during hydration. The clinker is then ground to produce cement (CSI).

2.3.1.1 Hydration of PC

The tricalcium and dicalcium silicate phases react with water to form calcium hydroxide and calcium-silicate hydrates (C-S-H), the product responsible for the strength of cement as shown below (Barron, 2010):

$$2(CaO)_3\,SiO_2 + 7H_2O \rightarrow (CaO)_3(SiO_2)_2 4H_2O + 3Ca(OH)_2 \qquad (2.1)$$

$$2(CaO)_2SiO_2 + 5H_2O \rightarrow (CaO)_3(SiO_2)_2 4H_2O + Ca(OH)_2 \qquad (2.2)$$

The tricalcium silicate reaction is the most important phase reaction for the first 28 days in terms of strength development. The dicalcium silicate reaction contributes to long-term development. The aluminate and ferrite phases also contribute to the hydration process, even though they exist in small amounts compared to the silicate phases. The aluminate phase hydration is a very rapid reaction and to slow this down, a small amount of gypsum is added.

2.3.1.2 Existing Studies on Self-healing Abilities of PC

Cementitious materials have shown a natural ability to heal cracks formed up to a certain extent. The natural self-healing of concrete is based on the following processes:

1) The swelling of hydrated cement paste near the crack surfaces
2) Hydration of un-hydrated cement near the crack surfaces leading to growth in the crack space
3) The reaction of calcium ions with carbonate ions of water to form calcium carbonate precipitates at the crack faces
4) Loose particles broken from the fracture surfaces blocking the crack faces
5) Solids originally in the water blocking the crack faces (Ramm & Biscoping, 1998)

However, calcium carbonate precipitation has been suggested as the most effective factor in accelerating autogenic self-healing (Edvardsen, 1999). Figure 2.1 demonstrates the natural self-healing mechanisms in cement (RILEM, 2013).

Research on autogenic healing of concrete started more than 20 years ago when it was shown that for concrete held in water, the Kaiser effect (absence of acoustic emissions during reloading) disappeared, confirming healing of cementitious materials upon hydration (RILEM, 2013). It is believed that the longevity of many old structures is due to the autogenic self-healing of concrete.

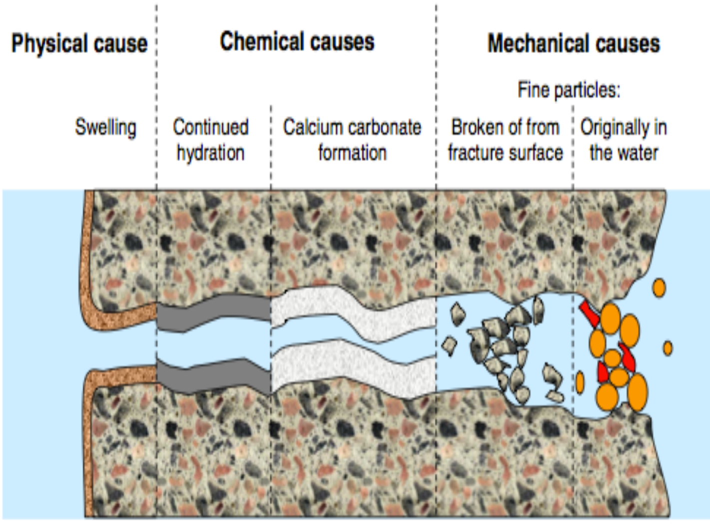

Figure 2.1-Causes of Natural Self-healing in cement

Numerous research articles have been published relating to the autogenic self-healing phenomenon in cementitious materials: Correlation between temperature and self-healing with varying crack widths (Reinhardt & Joos, 2003); In 1999 Edvardsen carried out a number of tests on concrete to investigate the effect of self-healing upon permeability of concrete and confirmed that precipitation of calcium carbonate is the most important process in reducing water leakage from the samples. He also concluded that the growth of $CaCO_3$ crystals depends highly on crack width and that it is surface controlled when initially exposed to water, whereas in later stages it is controlled by diffusion (Edvardsen, 1999).

More recently, a study by Ter Heide et al. (2007) investigated the effect of compressive stress, cement age at the time of cracking and crack width on the strength recovery and self-healing ability of concrete. Concrete specimens were cracked using a 3-point-bend test with a controlled crack mouth opening of 50 μm. A compressive force was then applied to close cracks and the samples were left to heal. They were tested again using the 3-point-bending to assess the mechanical properties of the healed crack after 2 weeks. The findings from these tests were that on-going hydration of the specimens was the main process responsible for crack healing. It was further concluded that cracks heal better if they are formed at an early age and a compressive stress is applied to close the crack surface. However it was found that the strength recovery is not dependent on the amount of compressive stress applied. (Ter Heide, 2007) .

2.3.2 Self-healing using Mineral Admixtures

The autogenic self-healing of concrete can be enhanced by incorporating minerals with certain properties. Existing works have included the incorporation of minerals such as blast-furnace slag, fly ash and expansive additives such as lime, bentonite clay and recently magnesium oxide. In this section existing work relating to some of these mineral admixtures will be reviewed with a focus on blast-furnace slag and magnesium oxide, discussing the reason for conducting experiments with these two additives.

2.3.2.1 Expansive Additives

Shrinkage upon hydration of cement pastes causes crack formation. Different expansive materials have been incorporated over the past 100 years to counteract this shrinkage effect. The main mechanisms of these additives are volume control and reducing the number of cracks. This section describes the details of various expansive additives.

(1) Calcium Sulfo-aluminate-based additives

These types of additives use the sulfate expansion property that is linked to the formation of ettringite when mixed with cement to overcome shrinkage. The formation of aluminate phases in the reactions to form ettringite is the most important factor for exploiting the expansive properties of these materials. CA (Calcium mono-aluminate) and C_4A_3S (Calcium sulfo-aluminate) react with $CaSO_4$ and CaO along with water to form ettringite (Odler & Colán-Subauste, 1999).

In 2007, Hosoda et al. carried out experiments on two types of calcium sulfo-aluminate (conventional and a newly developed high performance type) to investigate the effect on the self-healing of cracks created in concrete prisms. Specimens, restrained by steel bars, were cured for 7 days in wet conditions before being cracked. The results of further curing suggested that the new type of expansive additive produced the highest expansion of all mixes, followed by the specimen containing the highest content of the first type of additive, with samples containing no expansive additives showing almost no expansion. Figure 2.2 shows the results from one of the samples containing an expansive additive with an initial crack width of 0.3-0.4 mm that healed completely within 60 days. For normal concrete samples there was no sign of crack healing. It was concluded that the addition of sulfo-aluminate type additives enhances the self-healing ability of concrete specimens. However, a large amount is needed to contribute significantly, which would lead to high costs and an inferior quality of the concrete specimen without steel bars (Hosoda et. al, 2007).

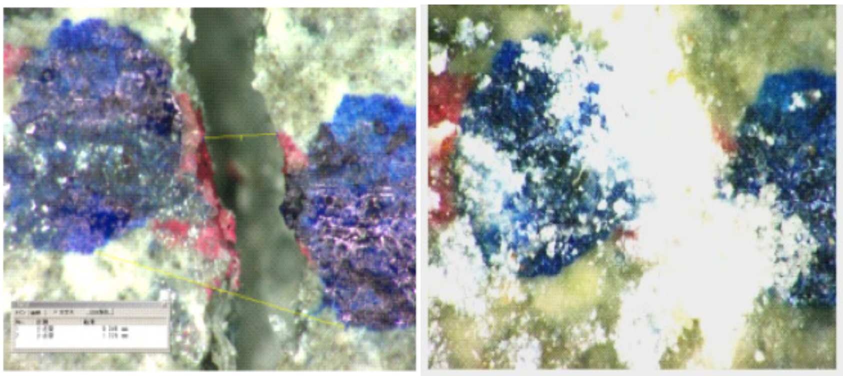

Figure 2.2- Sample at 7 days (just after cracking) and 60 days (Hosoda et al.)

Furthermore, a report by Telesca et al. discusses the effects of expansive and non-expansive calcium sulfo-aluminate additives on compensating shrinkage of cement pastes (Telesca et al., 2013). Three mixes, one containing OPC only, another a non-expansive CSA and the third an expansive CSA were cured for 90 days and subjected to shrinkage and compressive strength tests.

	4 hours	8 hours	1 day	7 days	28 days
CSA	23.3	27.0	35.8	53.3	61.8
MIX	7.8	18.2	30.0	39.4	54.7
OPC	-	2.0	21.5	49.5	61.0

Table 2.2- Compressive Strength Data for the Three Mixes (Telesca et al., 2013)

Table 2.2, demonstrates the compressive strength of the samples including CSA (both expansive and non-expansive) in MPa. The rapid formation of ettringite has yielded high initial compressive strengths in the CSA mixes. However at later stages OPC gained more strength due to its increased hydration whilst CSA and MIX both slowed down in strength development. It was also found that the MIX sample (containing the expansive CSA blend) produced the lowest level of shrinkage, followed by CSA and OPC (Figure 2.3).

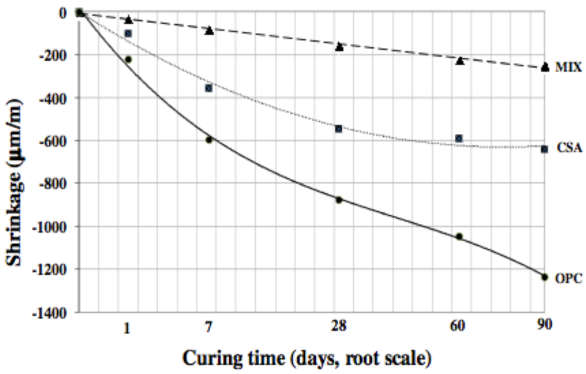

Figure 2.3-Shrinkage Level of the Mixes (Telesca et al.)

(2) Lime

The use of lime-pozzolan mortars dates back to many centuries ago. During the Roman times, these materials were used for the masonry construction of structures. Today lime is used with pozzolan to partially replace cement in mixes, with lime being very important for enhancing the performance of the mixes (Shi, 2001). Lime has been added in various forms in cement blends in the past, however it was only tested in the form of quicklime in 2001, in a study by Shi. Shi studied the effect of lime on strength development of lime-pozzolan mixtures. He also compared the effects of quicklime and hydrated lime on the mixtures. From this study it was concluded that the addition of lime under 20% does not affect the water requirement of the mix. However above 20% content, the addition of lime leads to a high water requirement as more hydrated lime is required to fill the pores of the pozzolan particles. It was also suggested that the addition of 20% lime resulted in the highest compressive strengths after 20 days (Figure 2.4).

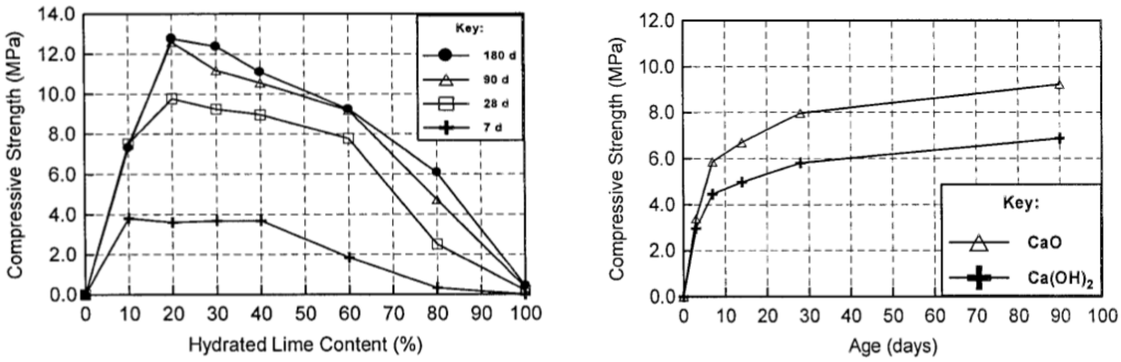

Figure 2.4- Effect of Lime Content and Lime Type on Compressive Strength (Shi, 2001)

This study also concluded that the addition of quicklime (CaO) instead of hydrated lime ($Ca(OH)_2$) resulted in higher strength developments with the difference becoming more noticeable between days 3-28 of curing. It was suggested that the addition of CaO to the mix instead of hydrated lime results in a faster pozzolanic reaction between the pozzolan and $Ca(OH)_2$ produced from the hydration of quicklime. Pozzolanic reactions lead to the formation of C-S-H gels, which are mainly responsible for the strength of cement pastes. It was also suggested that the hydrated lime-pozzolan mixture has a higher porosity compared to the quicklime-pozzolan mixture, which leads to a reduced strength. The limitation in the use of quicklime however, was the existence of $Ca(OH)_2$ in the structure even after 90 days, which leads to strength reduction.

More recently, quicklime was used in a study for enhancing the pozzolanic properties of fly ash, as fly ash has a slow pozzolanic reactivity on its own. Antiohos et al. published a report in 2008, studying the effect of quicklime on the properties of different fly ashes. Fly ash-cement blends with different contents of quicklime replacing fly ash were tested for strength development and reactivity as well microstructural changes. Two types of fly ash (High-calcium and Low-calcium) were used: 3% and 6%

quicklime were added to replace the high-calcium fly ash whereas for the low-calcium one, 5 and 15% quicklime contents were used. It was concluded that the addition of quicklime to a high-calcium fly ash-cement blend resulted in an increase in the solubility of SiO_2, releasing a higher percentage of silica into the hydrating mix and the addition of 3% quicklime resulted in the highest strength development with a positive effect on the reaction rate of fly ash. For the low-calcium fly ash-cement blend, activation only occurred at early stages of hydration (Antiohos et al., 2008).

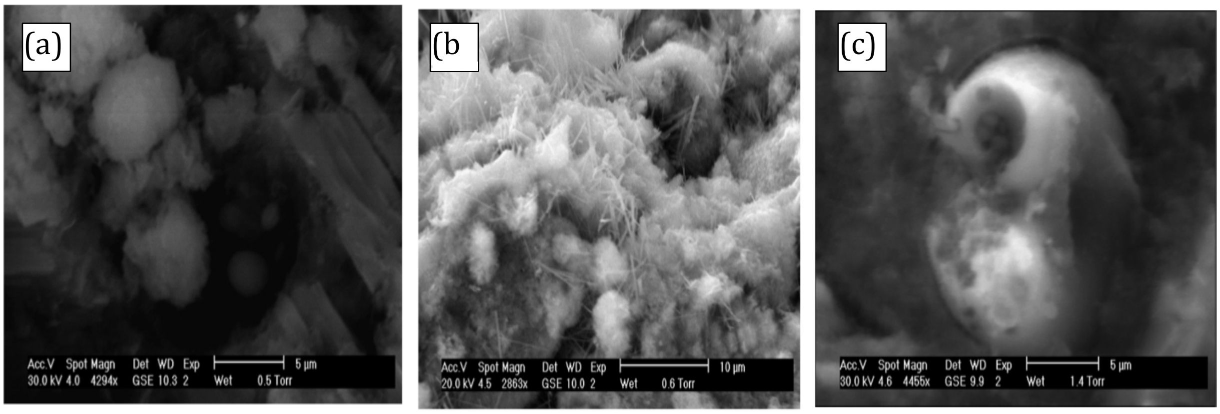

Figure 2.5- (a) Unreacted Fly Ash After 7 Days (With No Quicklime Added), (b) Formation of Hydration Products Precipitation After 7 Days in High-Calcium Fly Ash-Cement Blend (3% Quicklime), (c) Heavily Reacted Fly Ash After 90 Days (3% Quicklime) (Antiohos et al., 2008)

(3) Bentonite

Bentonite is composed of a mineral called montmorillonite (a form of calcined clay). It has been found to be abundant and relatively cheap to use as an alternative material to enhance the strength and durability of pastes, though its reactivity is known to be variable due to the variations in its mineralogy. Hydration of montmorillonite is thought to bring about swelling and expansion. Figure 2.5 shows a geo-material containing montmorillonite, due to which the material expanded by 15-18 times its dry state when tested by Ahn et al. (2009) with cement.

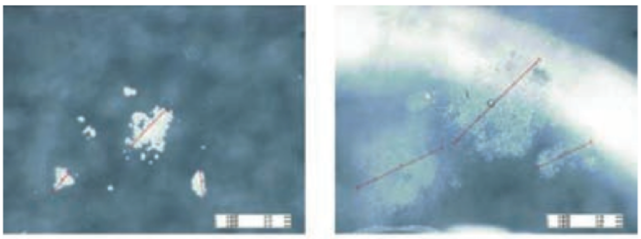

(a) Before water supply (b) After water supply

Figure 2.6-Swelling Effect of Montmorillonite Upon Hydration (Ahn et al., 2009)

A study by Targan et al. (2002) investigated the effect of the addition of up to 15% bentonite to PC pastes as well as up to 30% bentonite to fly ash-PC, colemanite ore waste-PC and coal bottom ash-PC mixtures with the percentage of FA, CW and BA kept constant at 10%, 4% and 10% respectively.

It was concluded that the addition of bentonite up to 15% on its own to PC mixtures resulted in high compressive strengths, whereas for mixtures with bentonite contents higher than 15% the compressive strength had reduced. It was also concluded that the increasing content of bentonite in presence of other admixtures resulted in a reduction in compressive strengths.

It was suggested that the high strengths for bentonite contents up to 15% were due to the increase in the pozzolanic reaction at early stages, whereas for contents higher than that, the increase in porosity of the structure due to bentonite counteracted the high pozzolanic contribution (Targan et al., 2002).

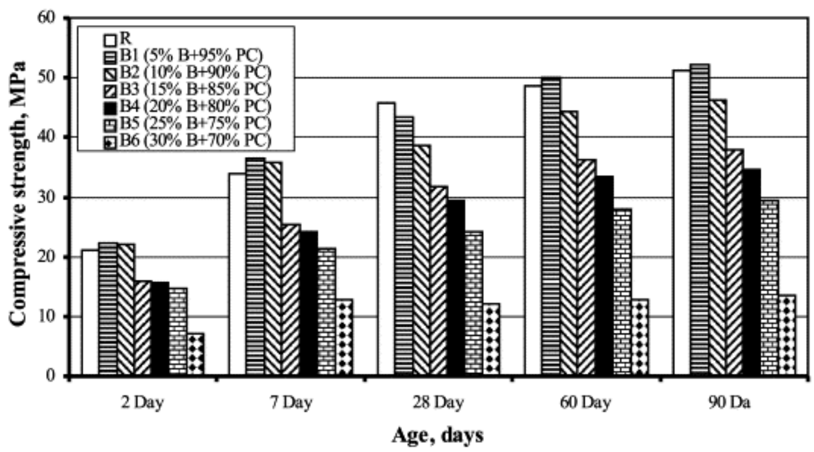

Figure 2.7- Compressive Strength of Concrete Containing PC and Bentonite (Targan et al.,2002)

(4) Magnesium Oxide

Magnesium Oxide has been recently suggested as an effective solution to autogenic self-healing as its hydration requires less water and the hydration product is more stable in the structure compared to other expansive mineral admixtures (Mo, Deng & Tang, 2010).

Known as Magnesia, it can be formed via 3 processes (Shand, 2006):

(1)Calcination of magnesite ($MgCO_3$)

$$MgCO_3 + Heat \rightarrow MgO + CO_2$$

(2) Heating of other minerals such as brucite or dolomite

$$Mg(OH)_2 + Heat \rightarrow MgO + H_2O$$

(3) Synthetic production from seawater or brine, for which the reactions involve the use of magnesium compounds such as ($MgSO_4$) to precipitate magnesium hydroxide by adding base.

Magnesia can be produced as follows:

(1) Caustic Calcined Magnesia (Light-burned): Calcination occurs at a decomposition temperature of between 600-800°C. This method produces magnesia with a high specific surface and therefore a very high reactivity level (European Commission, 2010).

(2) Hard-burned Magnesia: Calcination at temperature ranges of 1000-1200°C. This grade of magnesia has a very narrow range of reactivity (Shand, 2006).

(3) Dead-burned Magnesia (Sintered): At temperature ranges of 1600-2200°C. This grade has an even lower reactivity level compared to Hard-burned magnesia (Shand, 2006).

(4) Fused Magnesia: Produced at a temperature of 2800°C. Fused magnesia is not used in large amounts in Europe and is mainly used for refractory applications (European Commission, 2010).

Magnesium Oxide reacts with water upon hydration to form brucite as follows:

$$MgO + H_2O \rightarrow Mg(OH)_2$$

Brucite can react with CO_2 to form magnesium carbonate. These reactions are exothermic and result in a volume expansion of 118% (Li, 2010). Originally, due to the slow hydration nature of MgO in cement (as it is produced at 1450°C and is classified as dead-burned magnesia) its use in cement was very limited as otherwise it would lead to cracking (Mehta P. , 1978). However in 1980 a report was written suggesting that magnesium oxide can be used to control long-term thermal shrinkage (Mehta & Pirtz, 1980) and this result was later confirmed with the successful construction of the Baishan Dam in China in 1973 which was built from cement containing 4.5% MgO and contained no cracks after several years (Gao & Lu, 2008). Since then, many dams in China have been constructed using magnesium oxide as an expansive agent. The report written in 1980 also suggested that it is possible to produce MgO powders calcined to under the temperatures of between 900-950°C to be able to control the properties of MgO and produce grades of MgO other than dead-burned magnesia to use as expansive agents in compensating shrinkage.

A study was carried out by Mo et al. (2010) to investigate the effect of different calcination temperatures on the expansion property of magensium oxide-type expansive agent. Figures 2.8-10 show the SEM images of three MEA samples hydrated in water in order of increasing neutralisation time (46s, 325s and 1966s). For MEA-46 sample, all of the MgO has been fully hydrated after 7 days. For MEA-325 only 9.9% of the MgO is hydrated and MEA-1966 shows 0.98% of the MgO as hydrated after 7 days.

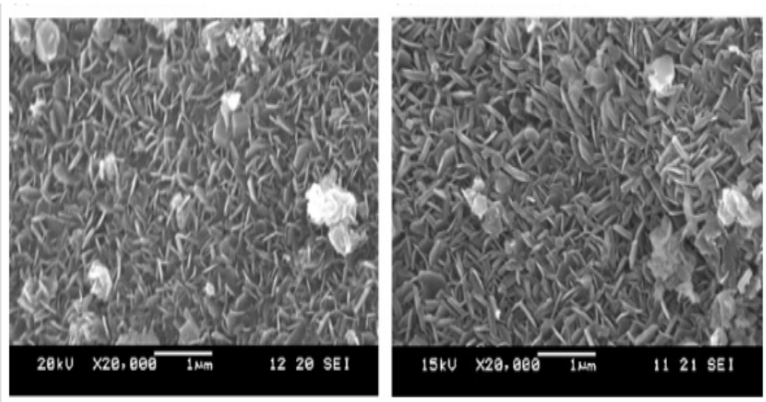

Figure 2.8- MEA-46 (Calcined at 900° C for 1 hour) on day 2 and day 7

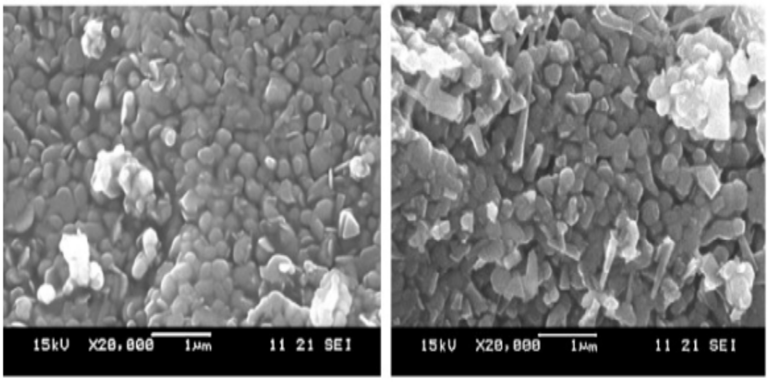

Figure 2.9- MEA-325 (Calcined at 1100° C for 1 hour) on day 2 and day 7

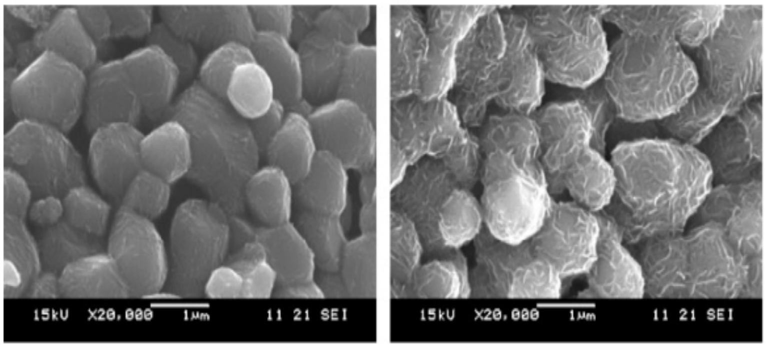

Figure 2.10-MEA-1966 (Calcined at 1300° C for 1 hour) on day 2 and day 7
(Mo et al., 2010)

It was concluded that for the MEA with lower activity, early age hydration is slow and therefore there will be a longer period before expansion is seen. Furthermore, two models were suggested for the hydration characteristics of magnesium oxide additives of different reactivity levels (Figures 2.11-12) (Mo et. al, 2010):

(1) For highly reactive MgO additives, hydration occurs at both the surface and the inner pores of the particles due to the highly porous structure of this type of MgO and the diffusion of water into these pores. This results in simultaneous hydration at the centre and the boundary of the grains. Upon the formation of magnesium hydroxide, it is partly accommodated by the existing pores in the core of the particles. Crystallisation in the core leads to expansion through the creation of growth pressure. However, crystallisation at the boundary causes the highest amount of expansion, as there is no space to accommodate the crystals. This model leads to accelerated rates of hydration and expansion due to the increase in the overall surface area caused by MgO grains breaking apart due to the expansive force present (Figures 2.11(a) and (b)).

(2) For less reactive MgO, as the specific surface area and the porous regions are reduced, there is less space available in the core of the particle to accommodate $Mg(OH)_2$ and a longer time is required to

break apart the MgO grains with a large enough expansive force. This results in a delayed acceleration in hydration and crystallisation (Figure 2.12(a) and (b)).

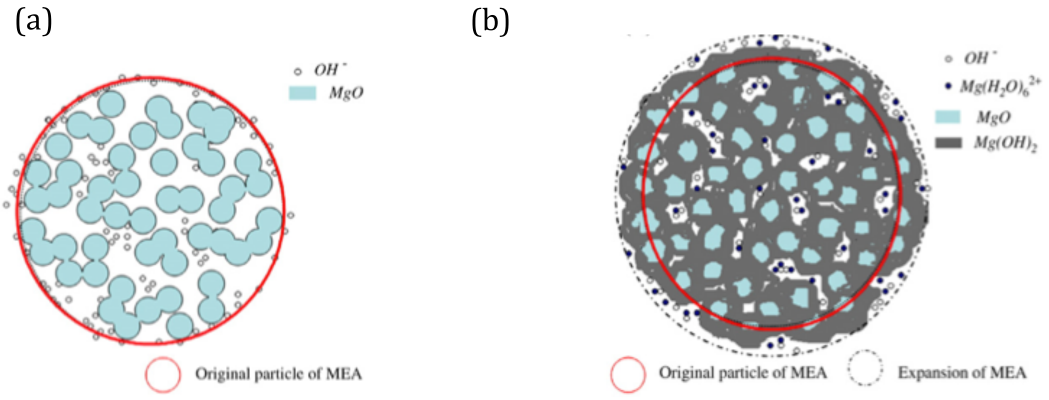

Figure 2.11-Expansion Model for Highly Reactive MgO

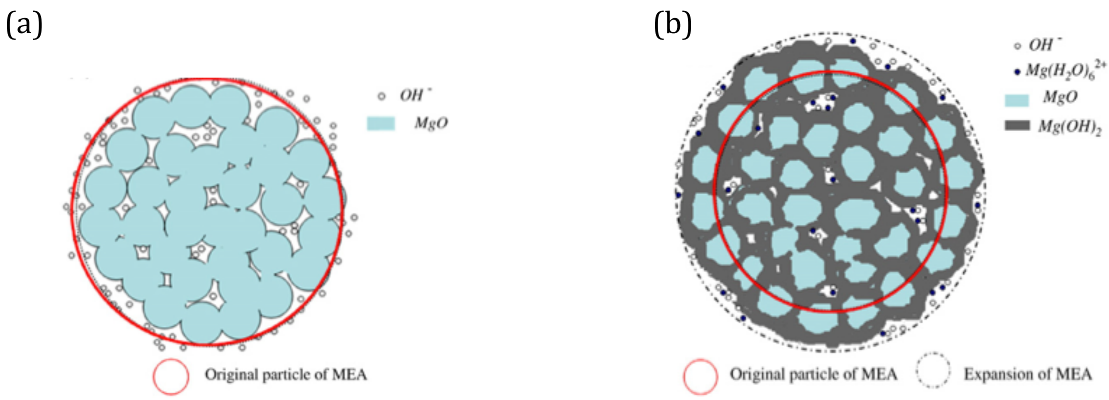

Figure 2.12-Expansion Model for a Less Reactive MgO

A recent study (Scientific American, 2008) has investigated the potential of using magnesium-based cement to absorb more CO_2 than is produced during its manufacture. However this technology has not been implemented to date due to complications. It can be seen therefore, that MgO does not only present the benefit of having expansive properties to compensate the shrinkage of concrete upon setting, but also presents environmental benefits as its calcination uses lower temperatures than those needed for OPC and it has the potential of acting as a source of CO_2 absorption in the future.

2.3.2.2 Ground Granulated Blast-furnace Slag

Blast-furnace slag is produced as a by-product during the manufacture of iron. The by-product has to be quenched to form granulates which are then ground. Unlike OPC, GGBS needs to be activated by alkalis and sulfates to form hydration products (Mortar Industry Association, 2012). GGBS has the same composition as PC in different proportions. The use of GGBS has lead to a reduction in CO_2 emissions of cement pastes as less cement is used in the mix when used in conjunction with GGBS. The reaction of GGBS with water is very slow. During the hydration of slag cement, PC hydrates first, providing the alkali environment needed to activate the hydration of GGBS. The activation of GGBS results in the formation of more hydration products that can act in tandem with the products from PC to have an improved effect on pore blocking as smaller pores form. The hydration of PC results in the formation of portlandite ($Ca(OH)_2$) and crystalline silicate hydrate gel (C-S-H). Portlandite often lacks in strength and is responsible for the quality of the paste formed. The presence of GGBS during hydration, leads to a reaction with portlandite to form products such as C-S-H (Oner & Akyuz, 2007). Hence more pores are filled with C-S-H in a slag cement paste than in a PC paste, which provides an enhanced microstructure.

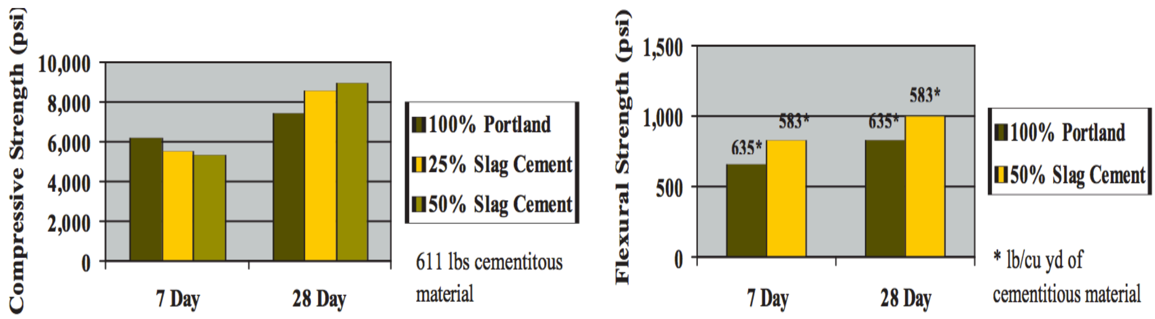

Figure 2.13- Effect of Slag Cement on 7-day and 28-day Compressive and Flexural Strength Development (Slag Cement Association, 2003)

Normally GGBS can be used to replace up to 50% of PC, however in special cases such as mass concrete, up to 80% PC has been successfully replaced (Regourd, 1980). This replacement generally results in a lower early-age strength development and a higher long-term strength. It has been suggested that the optimum strength of GGBS-PC is achieved when the content of GGBS is 50% (Neville, 1994). However there are conflicting reports as to whether the strength of slag reaches the same level as concrete containing OPC only and if so during which stage of curing (Barca, 2007). To date, very few studies have been carried out to study the effect of including MgO expansive additives in slag cement pastes.

A study by Van Tittelboom (2012), investigated the effect of using GGBS and fly ash on the autogenic self-healing property of concrete. This paper suggested that due to the slow hydration of GGBS, its self-healing ability would be higher as upon cracking the particles of GGBS that had not reacted before could be activated to seal the crack. Samples of PC in combination with 50%, 75%, 80% GGBS and 30% and 50% fly ash with a water-to-binder ratio of 0.4 were tested for self-healing properties and mechanical properties. From the tests it was concluded that the addition of slag and fly ash improve the self-healing of concrete providing that hydration is the main mechanism. Of the two admixtures, blast-furnace slag had shown the most improvement. However, no notable differences were seen between the mechanical strength regain of the different mixes, although it was concluded that the samples with samller crack widths had shown a better strength regain.

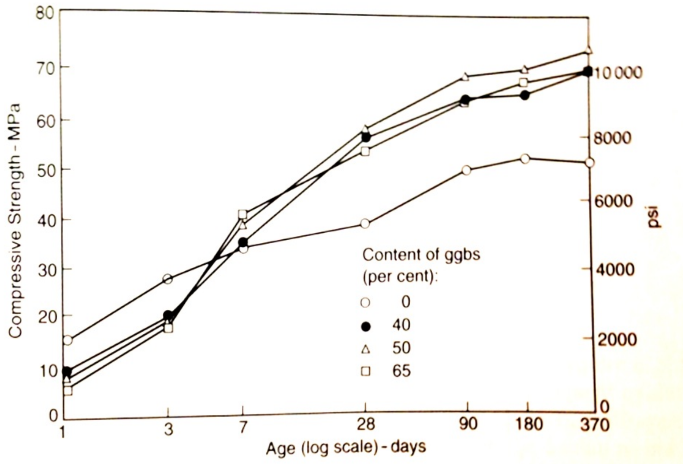

Figure 2.14-Compressive Strength Development of Concrete for GGBS at Different Contents (Neville,1994)

Despite all the positive aspects of slag, it is found that the inclusion of GGBS leads to carbonation shrinkage in concrete due to a lower $Ca(OH)_2$ content in comparison with plain Portland cement. Recent studies on blast-furnace slag has involved the use of encapsulated sodium monofluorophosphate to improve the quality of interfacial transition zone when carbonation shrinkage in slag-rich concrete occurs (Ahmad, 2011).

2.4 Conclusion

Recent research on addition of MgO has shown great potential for enhancing the self-healing properties of cementitious materials. This type of expansive additive has offered advantages over traditional expansive additives such as the ability to design the expansion properties of MgO as proven by Mo et al. (2010), as well as the lower amount of water required for the formation of brucite and higher stability under higher temperatures (Mo, Deng, & Al-Tabbaa, 2014). It also offers several benefits over PC such as the improved ability to sequester CO_2, higher resistance of the precipitates (carbonated and hydrated) in harsh environements and the enhanced ability to accommodate impurities such as industrial by-products (Unluer & Al-Tabbaa, 2013).

Given the advantages of using GGBS such as strength and durability enhancing characteristics in addition to the environmental benefits it offers (Siddique & Bennacer, 2012), it is beneficial to study the effects of MgO at different reactivity levels along with GGBS on the self-healing of cement mixes.

3 Materials and Experimental Procedures

3.1 Introduction

In this section of the report the materials used for the experiments are detailed along with descriptions of the experimental procedures and methods used to analyse the self-healing progress of the different samples.

3.2 Materials

The materials used for the experiments were ordinary Portland cement, two types of MgO (up to 7%) and GGBS (50%) along with a superplasticiser to improve the performance of the hardening fresh paste (reducing the water to cement ratio of the mix). The water-to-binder ratio for each mix was determined using standard consistency tests.

The following table summarises the chemical composition of each material:

Oxide Type (%)	Portland Cement	MgO N50	MgO 92/200	GGBS
SiO_2	19.50	---	2.25	36.1
Al_2O_3	4.90	---	0.22	12.5
CaO	63.60	0.5	0.87	40.1
Fe_2O_3	3.10	0.03	0.53	0.4
MgO	0.90	97.70	93.18	9.5
SO_3	3.30	0.80	---	---
Na_2O	---	---	---	0.4
K_2O	---	---	---	---
TiO_2	---	---	---	---
$CaCO_3$	---	---	---	---
Mn	---	0.002	---	---
Cl	---	0.10	---	---
Loss on ignition	2.10	5.40	2.59	---

Table 3.1- Summary of Chemical Composition of Materials (From Suppliers' Datasheets)

3.2.1 Portland Cement

The type of PC used was CEM I (52.5N) provided by Hanson, UK Ltd to comply with the requirements of BS EN 197-1.

3.2.2 Magnesium Oxide

MgO N50 and 92/200 were selected as the two types of MgO. MgO N50 is a type of light magnesium oxide (highly reactive) produced synthetically from seawater or brine. MgO 92/200 is produced from the calcination of magnesite and is less reactive than N50. Both types of magnesia were supplied by RBH (Richard Baker Harrison Ltd), with N50 and 92/200 having a specific gravity of 3.6

g/cm^3 and 3.02 g/cm^3 respectively. Magnesium Oxide reacts with water to form brucite ($Mg(OH)_2$) which results in expansion and can further react with CO_2 to produce magnesium carbonate precipitates. In presence of Si sources (slag and fly ash) Magnesium-Silicate Hydrates could form, which could enhance the strength of the structure.

3.2.3 Ground Granulated Blast-furnace Slag Cement

GGBS was supplied by Civil & Marine Ltd., a Hanson related company, with a specific gravity of 2.9 g/cm^3 to conform to BS EN15167-1 for use of GGBS in concrete.

3.2.4 Superplasticiser

The use of a superplasticiser helped to enhance the cohesion of cement mixes. For the experiments Sikament 700, supplied by Sika Ltd was chosen, which complies with the requirements of BS EN 934-2. Using a superplasticiser helps achieve better self-healing results.

3.3 Mix Design

Experiments were carried out on 11 mixes, containing MgO, slag and PC in different proportions. For each sample, standard consistency tests were performed to determine the water to binder ratio. The amount of superplasticiser was kept constant at 0.3% of the total powder used. Table 3.2 lists the 11 types of mixes with their composition and the water to binder ratio required to create them.

Mix	PC (%)	MgO N50 (%)	MgO 92/200 (%)	GGBS (%)	Water to binder ratio
1	100	---	---	---	0.29
2	97	3	---	---	0.31
3	95	5	---	---	0.32
4	93	7	---	---	0.34
5	97	---	3	---	0.29
6	95	---	5	---	0.30
7	93	---	7	---	0.31
8	48.5	---	3	48.5	0.28
9	47.5	---	5	47.5	0.29
10	46.5	---	7	46.5	0.30
11	50	---	---	50	0.28

Table 3.2- Mix Proportion of Samples

Table 3.3 shows the provisional sample preparation and testing timetable for every mix. In addition to the tabulated tests, X-Ray Diffraction analysis was performed for Mix 1,3 and 6 from April-May. The mixes were prepared to be tested for compressive strength, mechanical strength recovery and crack width recovery.

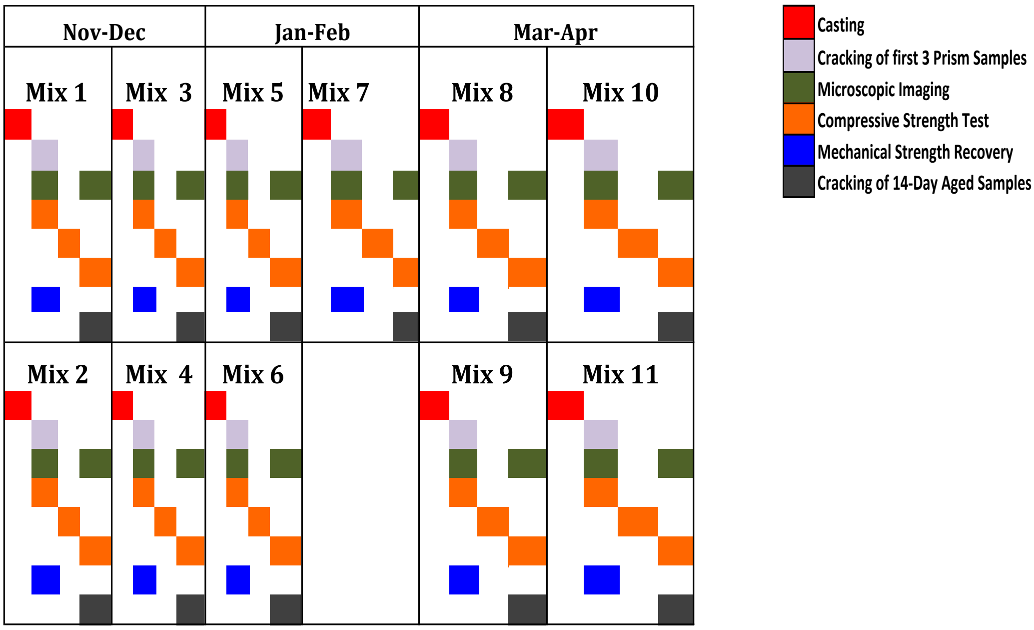

Table 3.3-Provisional Sample Preparation and Testing Timetable

3.4 Preparation of Samples

Six prism samples of dimensions 40x40x160 mm and nine cube samples of dimensions 40x40x40 mm were produced for each mix. 4000 g of powder in total (PC plus any additive) was needed for each mix to produce the number of samples required.

At first, the water to binder ratio for each mix was determined using the Vicat apparatus. The PC powder was then mixed with other minerals using a high power food mixer at a speed of 190 rpm under dry conditions for 1-2 minutes. It was then made sure that the powder is homogeneous and water was added for approximately 5 minutes, occasionally stirring the bowl manually to scrape off any dry particles.

The mix was then poured into the prism and cube moulds. The moulds were lubricated with oil beforehand to facilitate the de-moulding process. After the moulds were filled, they were manually vibrated to ensure there were no gas bubbles entrapped in the mix, which could affect the integrity of the structure. The surfaces of the moulds were flattened, covered with cling film to avoid loss of moisture from the samples and the samples were left to dry for 24 hours before de-moulding. The room temperature was kept at 20°C with a relative humidity of 60. The samples were placed in a curing tank filled with tap water to encourage self-healing.

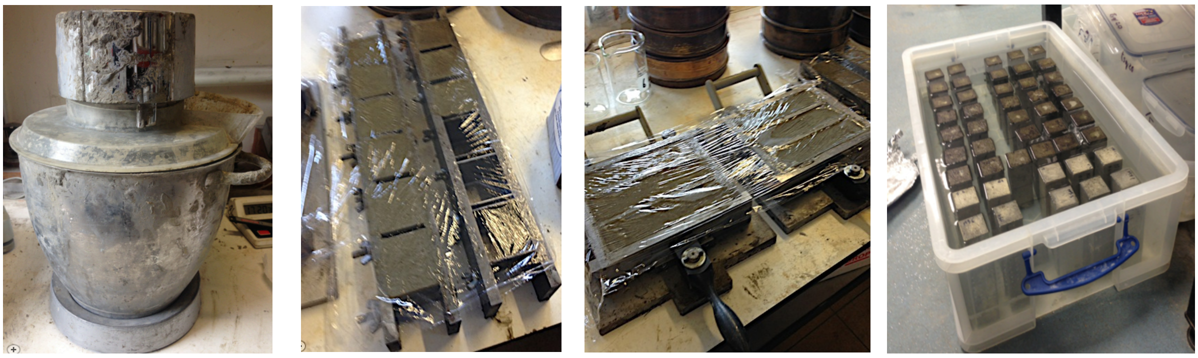

Figure 3.1-Sample Preparation

3.5 Experimental Methods

Tests were carried out to:

1) Assess the intrinsic self-healing ability of PC without the addition of MgO or GGBS in terms of visible crack sealing, compressive strength gain and mechanical strength regain after cracking at different ages
2) Compare (1) with the self-healing ability of PC including MgO N50 or 92/200 of different contents
3) Analyse the effect of replacing 50% of PC with GGBS with and without 3-7 % MgO 92/200 content

For each mix three prisms were cracked on the first day after de-moulding and placed in a curing tank for a period of 14 days to heal, while the remaining three were cured for 14 days without a crack and then cracked to compare to the mechanical strength of samples cracked on day 1. Microscopic imaging was used to monitor the healing of the cracks from day 1-14. The cube samples were used to evaluate the compressive strength development of each mix. Therefore, three cube samples were tested before curing, with another three tested on day 3 and the remaining three on day 14.

3.5.1 Standard Consistency Test

To determine the water-to-binder ratio of each mix, standard consistency tests conforming to requirements of ASTM C-187 and BS-12 were carried out as follows: 500g of the cement powder was mixed using the mixer and a measured quantity of water was added and the sample was mixed homogeneously. The cylindrical mould of the apparatus was then filled with the mix and the surface of the paste levelled. A plunger with 10mm diameter and 50 mm length was then brought into close contact with the surface of the mix and then released into the mix. The standard consistency was achieved when the plunger settled to 6±2 mm above the bottom surface in 30 seconds. The test was therefore repeated with modified quantities of water to achieve the right level.

Figure 3.2-Standard Consistency Test Using the Vicat Apparatus

3.5.2 Compressive Strength Test

A 250kN compressive strength test cell was used to measure the compressive strength of cube samples. Testing was carried out on days 1,3 and 14. The cubes were taken out of the curing tank, dried, weighed and measured each time before being placed between two steel plates. The test setup was set to 40 mm cubic testing, using frame 2 in the structural lab of the Engineering Department. The test was done according to the specifications of BS EN 196-1:2005 with a speed of 2.4 kN per second. The top plate made contact with the surface of the sample, followed by continual loading to determine the maximum compressive strength. When this strength was reached, the samples crushed and the final load reached was recorded.

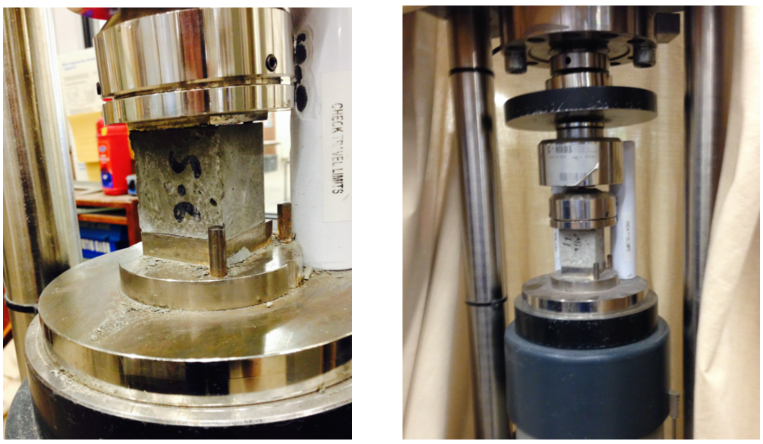

Figure 3.3-Compressive Strength Test Setup

3.5.3 Mechanical Strength Test (Three-point Bend Test)

To determine the extent of mechanical or flexural strength recovery of the samples due to self-healing and curing, it was necessary to create controlled cracks on the prism samples using a three-point bend test machine. Samples were cracked on day 1 and 14. The crack widths of 1-day cured samples were then measured using a microscope before curing the samples for a further two weeks.

On day 14 the samples were taken out to perform microscopic imaging before carrying out another three-point bend test to determine the strength recovery percentage.

Figure 3.4-Three Point Bent test Setup

For each test, the sample was marked at mid-span on one side and where the supports were going to be, on the other side. The distance between the supports was taken as 125mm. 2kN and 30kN capacity Instron machines were used for the tests. The sample was placed on the supports with the loading shaft slowly brought close to the top surface of the prism, aligned with the mark at its mid-span. The prism was then loaded by the shaft until a crack was formed, at which point the test stopped and data recorded provided information on corresponding loads and displacements at various points throughout the test. Even though the tests were carried out to form controlled cracks within the samples, due to the brittleness of some of the concrete samples, they completely separated. Therefore after performing the test, when placed upright in the curing tank to heal for 14 days, a small pressure was applied, enough to make contact between the two surfaces of the broken samples to initiate the healing process.

3.5.4 Microscopic Imaging

To be able to assess the healing of cracks, a digital microscope placed in the materials laboratory was used to measure crack widths of samples on day 1 and day 14. The digital microscope used was GXCAM 1.3 type microscope. Before capturing images, the microscope was calibrated at the start of each session.

3.5.5 X-Ray Diffraction Pattern Analysis

For XRD, healed specimens of Mix 1, 3 and 6 were taken for analysis. The healed materials on the surface of the cracks were scraped off and ground using a pestle. The ground samples were then passed through a 75 micron sieve and collected in 3 different containers. Acetone was then poured into the containers to stop further hydration of the samples. After a week, the excess acetone was drained off and the containers were placed in a vacuum drier for a week. A small amount of each sample was positioned in the central circular section of an XRD slide and the surface was levelled using a glass slide (Figure 3.5). A Siemens Diffraktometer (Figure 3.6) was used with safety features such as hazard lights to minimise the risk from X-ray exposure. The slide was placed in the machine and measurements were taken to produce graphs.

Figure 3.5- XRD Slide

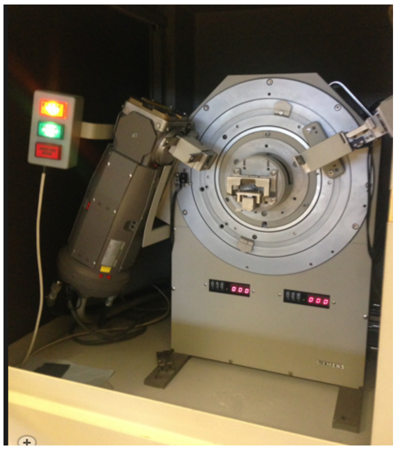

Figure 3.6-XRD Machine

For each mix the following parameters were defined:

2θ Range = 5-60°

Step Rate = 1 Step/Second

Step Size = 0.05°

3.6 Conclusion

Two types of MgO, N50 and 92/200 (light-burned and calcined at high temperatures) were chosen as the expansive mineral additives. OPC was chosen as the base material and 3-7% MgO was added to OPC for the analysis of the effect on self-healing of concrete. GGBS was used as the second type of mineral additive. This was added to OPC at a 50:50 ratio to compare the results to that of 100% OPC. Finally, 3-7% MgO 92/200 was added to the mix of GGBS and OPC. Cube and prism samples were prepared for testing. Cube samples were used on days 1,3 and 14 of curing for compressive strength tests and the prisms were used to create a crack using three-point bend tests on day 1 and were cured to check for mechanical strength recovery and crack healing on day 14. Some prism samples were also cracked on day 14 after being placed in curing tanks to compare the effect of early age cracking to the cracking of samples at later ages. The healing of the cracks was also observed using digital microscopy. To analyse the healed material in the samples, XRD analysis was used to identify the compounds in Mix 1, 3 and 6.

4 Results and Discussion

4.1 Compressive Strength

The results of the compressive tests are tabulated in Table 4.1 and were used to construct figures 4.1-4.4.

	Day 1 Average Strength (MPa)	Day 3 Average Strength (MPa)	Day 14 Average Strength (MPa)
Mix 1	37.03±8.1%	69.88±0.9%	87.64±3.0%
Mix 2	27.38±0.8%	56.78±2.5%	78.33±1.6%
Mix 3	23.94±4.7%	50.59±3.9%	72.38±1.2%
Mix 4	17.08±1.8%	35.65±8.8%	53.93±8.0%
Mix 5	49.46±7.5%	71.35±3.3%	73.09±4.0%
Mix 6	43.03±2.9%	72.06±5.7%	77.30±1.1%
Mix 7	37.40±2.5%	67.60±2.7%	68.77±2.9%
Mix 8	16.70±3.1%	29.19±6.1%	52.41±2.8%
Mix 9	20.96±4.1%	30.64±1.3%	55.08±5.3%
Mix 10	14.51±1.7%	34.15±5.1%	55.63±12.3%
Mix 11	20.22±1.4%	44.68±3.5%	74.83±4.8%

Table 4.1- Compressive Strength Development of Mixes (Day 1-14)

The addition of MgO and GGBS reduced the compressive strength of the samples. There was a bigger contrast between the compressive strength developments of MgO N50 at different contents compared to MgO 92/200. Figure 4.1 suggests that the addition of 3% MgO N50 yielded the highest compressive strength from the three MgO N50 mixes and figure 4.2 suggests 5% MgO 92/200 yielded the highest value. MgO and cement hydrate independently, therefore for MgO N50, lower compressive strength values are expected compared to 100%PC mixes, as the higher the content of N50 the higher the formation of brucite on day 1, which is known to be weaker than portlandite and C-S-H. It is expected for MgO N50 to see a pattern of compressive strength development similar to 100% PC, only at lower strengths with increasing content, as seen in figure 4.1, as the hydration of N50 happens at an early age and therefore is not contributing to the strength development after that. It could also be argued that there was a delay in the reaction of MgO for both types, as it has been suggested that in presence of both cement and MgO, hydration of cement is more favoured in comparison to MgO (as portlandite is more soluble than brucite). Therefore there was a delay in the start of hydration of both MgO N50 and 92/200, and unreacted MgO resulted in lower strengths. MgO 92/200 is known to be less reactive than N50. Therefore it is expected for some hydration to occur in the first few days (only a small amount) with the products only forming around the grains of MgO, followed by a period of slow hydration before rapidly expanding. From the compressive strength graph of MgO 92/200, it is clear that during the first 3 days, some hydration occurred, however from day 3 onwards the hydration rate of MgO 92/200 reduced, indicating the slow reactivity of this type of MgO (figure 4.2) and hence the slow strength development.

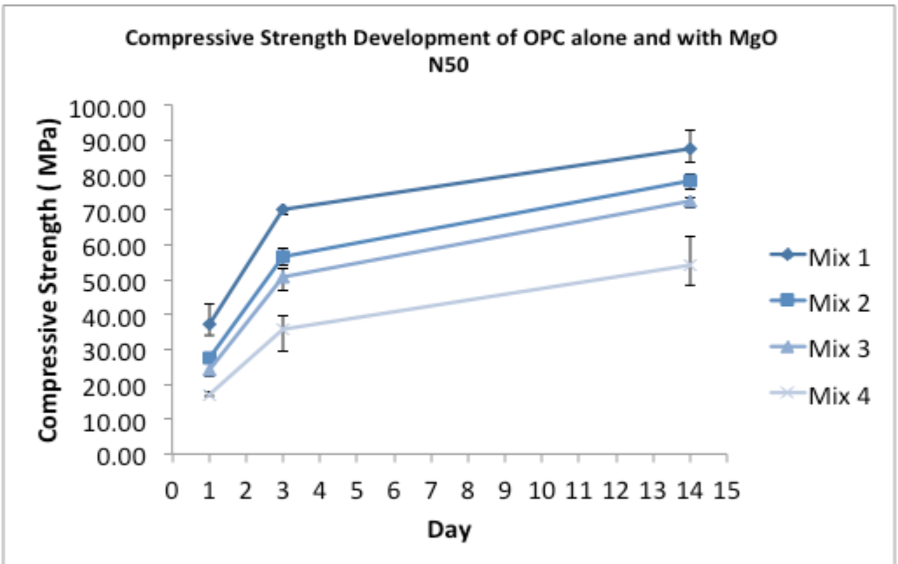

Figure 4.1- Compressive Strength Development of OPC with MgO N50

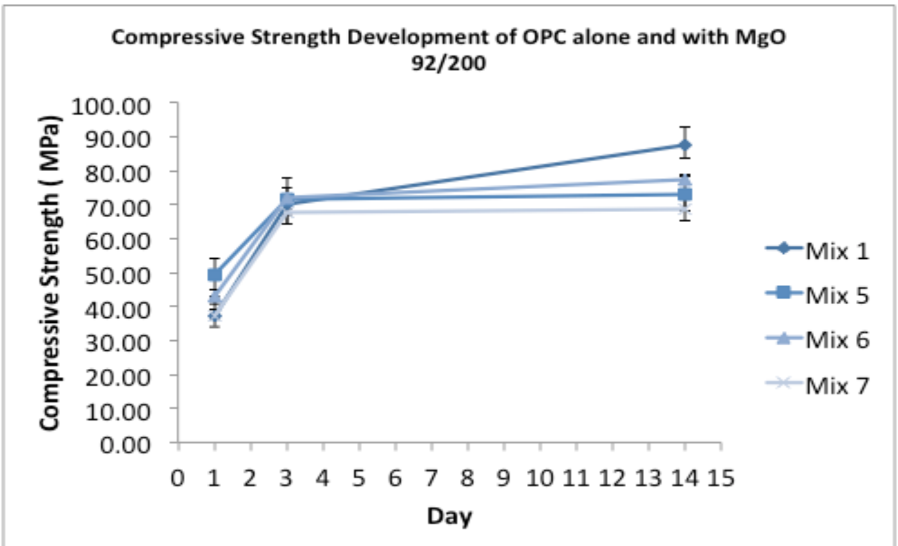

Figure 4.2- Compressive Strength of OPC with MgO 92/200

Comparing the compressive strength development of 100% PC and 50-50 PC-GGBS (figure 4.3), it is clear that the early-age strength of PC-GGBS is much lower than 100% PC, which confirms the theory that GGBS has a slow hydration rate at first, as it needs to be activated by alkali such as portlandite that only forms once PC has been hydrated. Once activated, GGBS hydrates to form C-S-H, contributing to the long-term strength of the samples. However during the first 14 days, GGBS has yielded a lower compressive strength, though from day 3-14 an increase in the rate of development was observed compared to 100% PC. The addition of MgO 92/200 to GGBS-PC mix resulted in samples with lower compressive strengths than MgO-PC mixes (figure 4.4). This could be due to the partial replacement of PC with GGBS, though the addition of GGBS increased the compressive strength of these samples from day 3-14, contrary to the insignificant change in strength development of MgO 92/200-PC mixes from day 3-14. This could be due to the activation of GGBS by $Mg(OH)_2$ formed in addition to portlandite, which forms more C-S-H. Although the amount of brucite is decreased, there could be some hydrotalcite formed $Mg_6Al_2(CO_3)(OH)_{16} \cdot 4(H_2O)$ which could later contribute to increased strength.

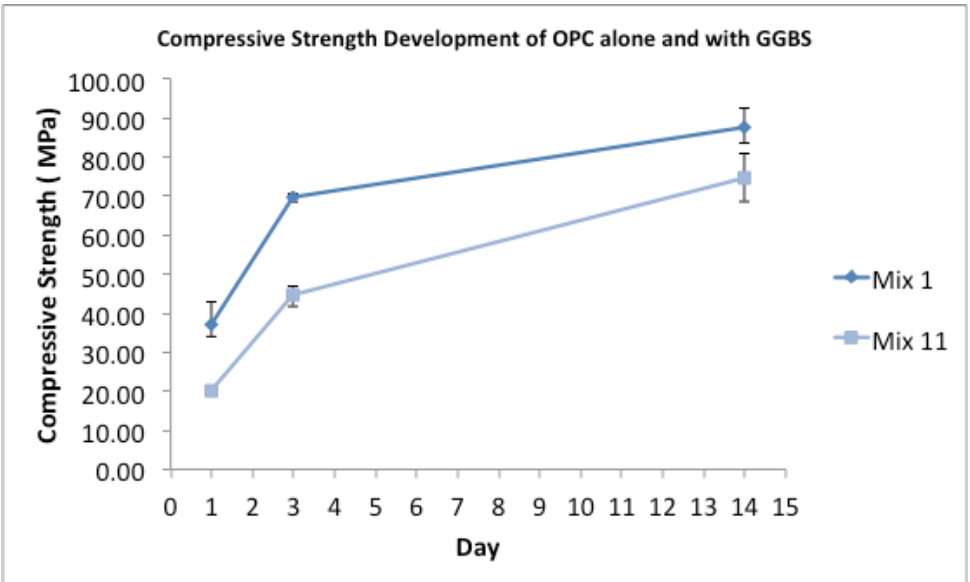

Figure 4.3- Compressive Strength of OPC with GGBS

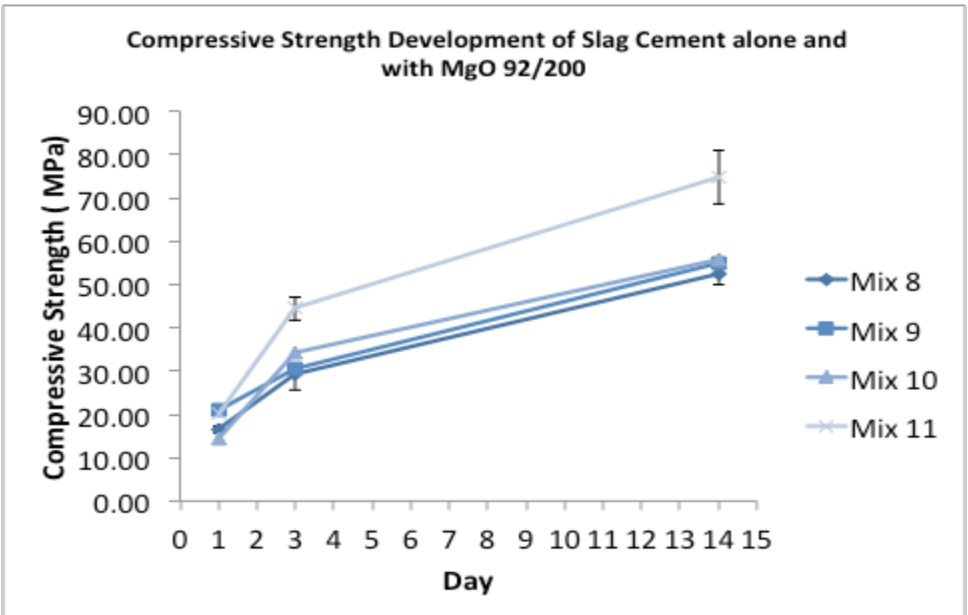

Figure 4.4- Compressive Strength Development of Slag Cement with MgO 92/200

4.2 Microscopic Imaging

4.2.1 Healing of Cracks & Crystallisation

Figures 4.5-4.15 show the microscopic images taken of Mixes 1-11 on Day 1 and Day 14 of curing. The addition of MgO N50 and 92/200 to OPC has shown the best crack recovery with time, with some samples in Mix 2-7 showing complete sealing of cracks in some parts. Therefore, MgO has acted to expand and heal the cracks formed upon hydration at a faster rate than PC via the formation of $Mg(OH)_2$ and magnesite crystals. The addition of 5% and 7% MgO 92/200 also resulted in complete crack recovery in some parts of some of the samples. The addition of MgO 92/200 and GGBS to OPC resulted in a higher crystallisation growth rate than MgO N50.

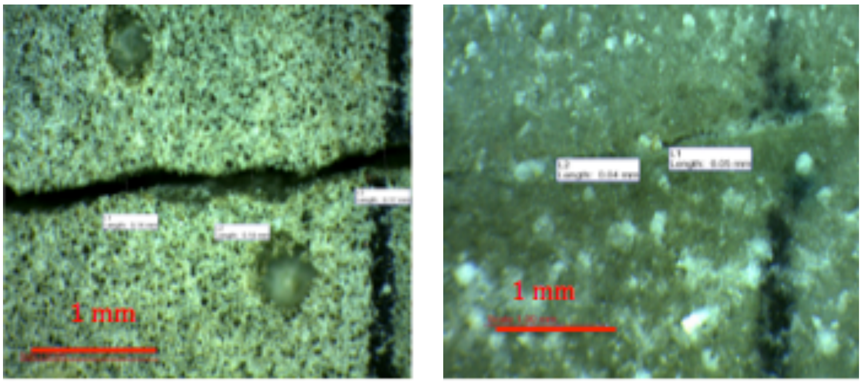

Figure 4.5-Digital Microscopy of 100% OPC on Day 1 and Day 14

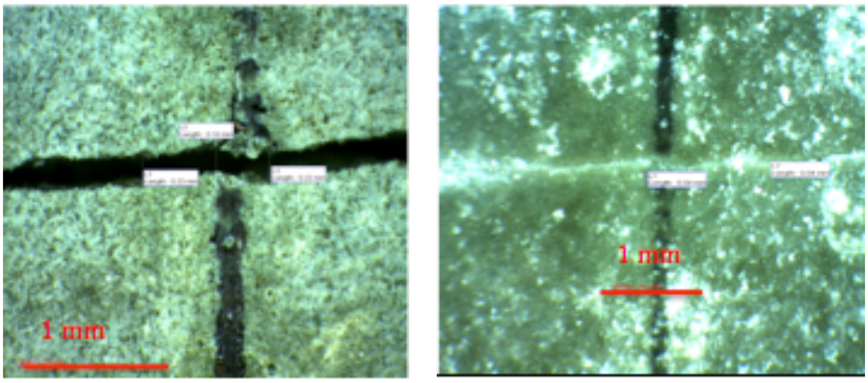

Figure 4.6- Digital Microscopy of OPC- 3% MgO N50 on Day 1 and Day 14

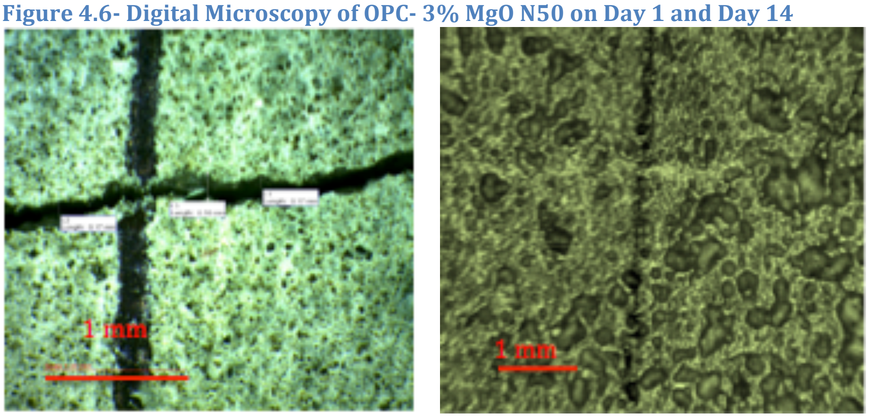

Figure 4.7- Digital Microscopy of OPC-5% MgO N50 on Day 1 and Day 14

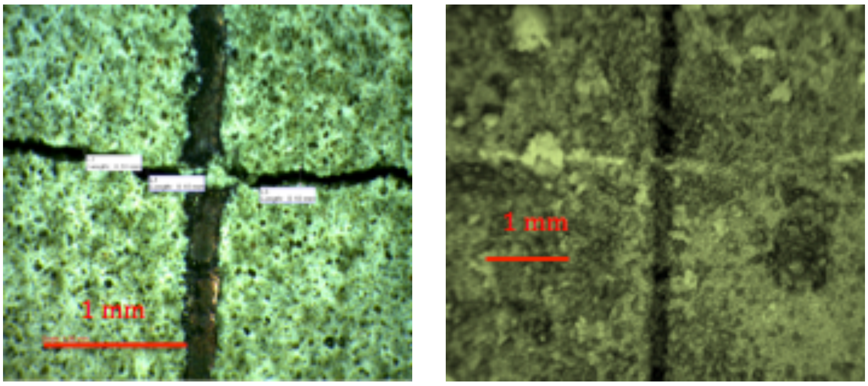

Figure 4.8- Digital Microscopy of OPC-7% MgO N50 on Day 1 and Day 14

The addition of MgO N50 has enhanced the crack sealing process in comparison with figure 4.5. Figures 4.6-8 show crystalline growth between the crack faces. Comparing this to figures 4.9-11, it can be deduced that the degree of crystallisation for OPC with MgO N50 is lower than that for OPC with MgO 92/200. This is in accordance with existing results: MgO N50 is a highly reactive MgO type; Therefore it has a faster hydration rate than MgO 92/200 and this means that it reacts with water and CO_2 very quickly to form brucite and magnesium carbonate. Therefore precipitation happens at early stages of curing and therefore less crystallisation occurs at later stages, as less reactive MgO remains in the sample to react with water. Therefore on day 14, MgO 92/200 exhibited a higher degree of crystallisation than MgO N50. The effect of the degree of crystallisation and crack healing on mechanical strength recovery is covered in the mechanical strength results section.

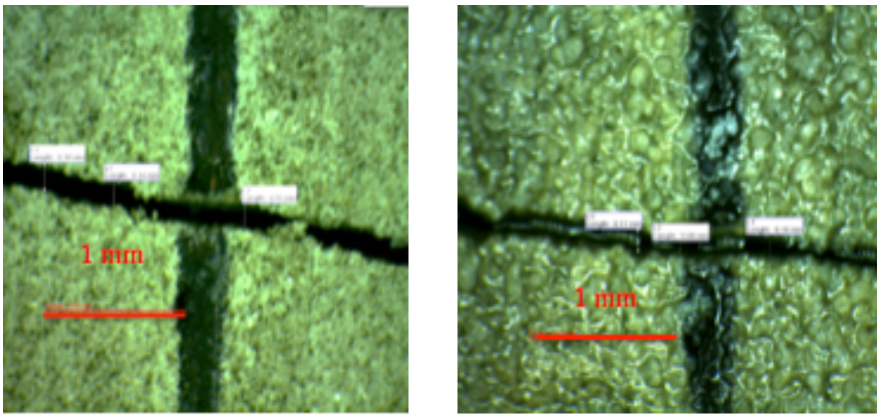

Figure 4.9- Digital Microscopy of OPC-3% MgO 92/200 on Day 1 and Day 14

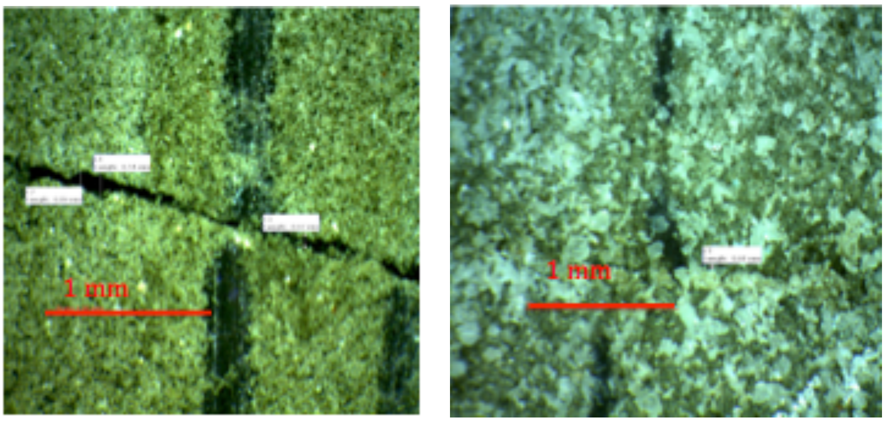

Figure 4.10- Digital Microscopy of OPC-5% MgO 92/200 on Day 1 and Day 14

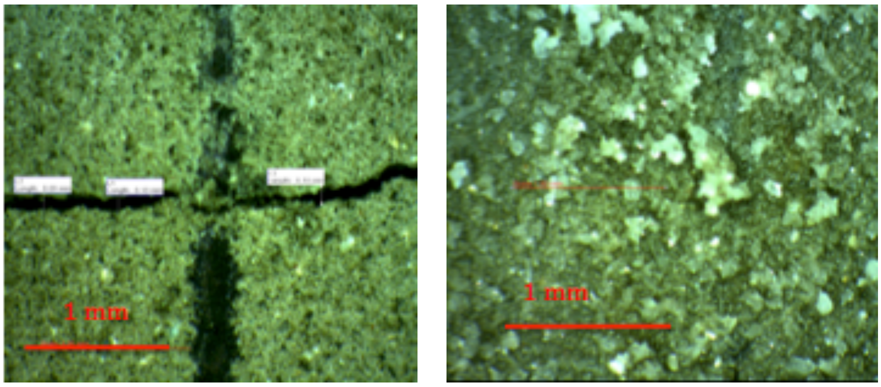

Figure 4.11-Digital Microscopy of OPC-7% MgO 92/200 on Day 1 and Day 14

The addition of MgO 92/200 to slag cement has produced a high degree of crystallisation. This could be due to both the presence of MgO 92/200 and GGBS, and comparing the images to the results for MgO 92/200 added to OPC (figures 4.9-11), it could be concluded that GGBS has contributed to the crystallisation process. This is confirmed in figure 4.15, demonstrating the results for the healing of slag cement in the absence of MgO 92/200. During the curing of Mix 8-11, GGBS had to be activated first using the product of OPC hydration (Portlandite). Therefore it was expected to see a delayed healing in samples containing GGBS as the full formation of calcium silicate hydrates (C-S-H binding gel) is delayed, and less brucite is formed as $Mg(OH)_2$ is also used to form C-S-H, though hydrotalcite could be formed instead which results in crystallisation as well as magnesite. Overall a lower level of healing at the early stages would be expected. It is expected for the portlandite formation to decrease with the activation of slag as $Ca(OH)_2$ is used up by slag to form C-S-H. Very few studies have been carried out incorporating MgO into a slag cement mix.

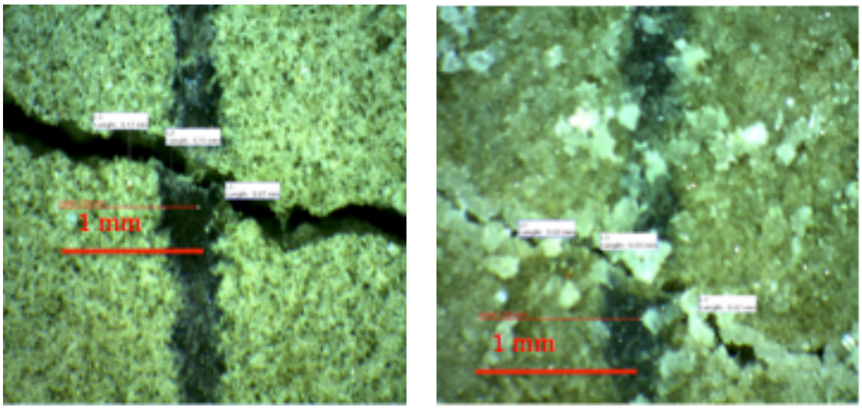

Figure 4.12- Digital Microscopy of slag cement-3% MgO 92/200 on Day 1 and Day 14

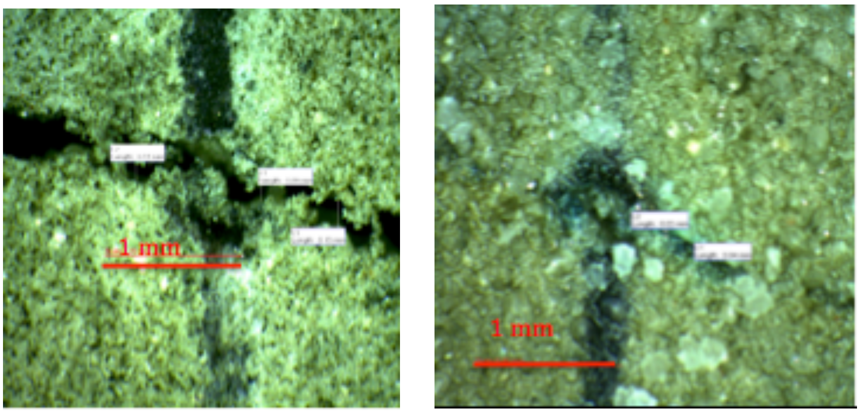

Figure 4.13- Digital Microscopy of slag cement-5% MgO 92/200 on Day 1 and Day 14

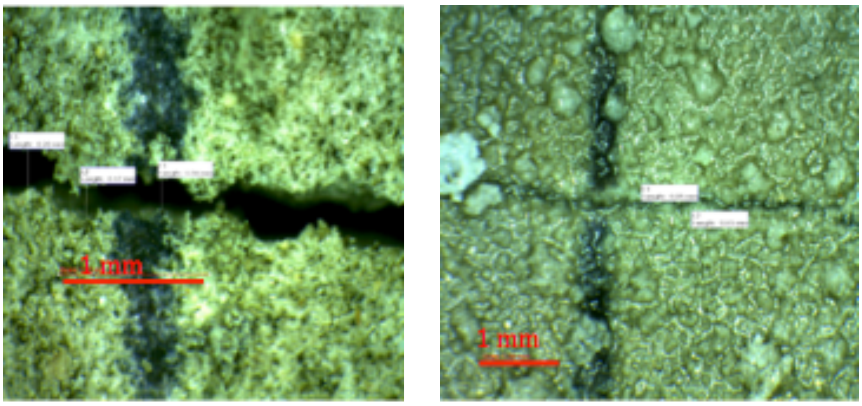

Figure 4.14- Digital Microscopy of slag cement-7% MgO 92/200 on Day 1 and Day 14

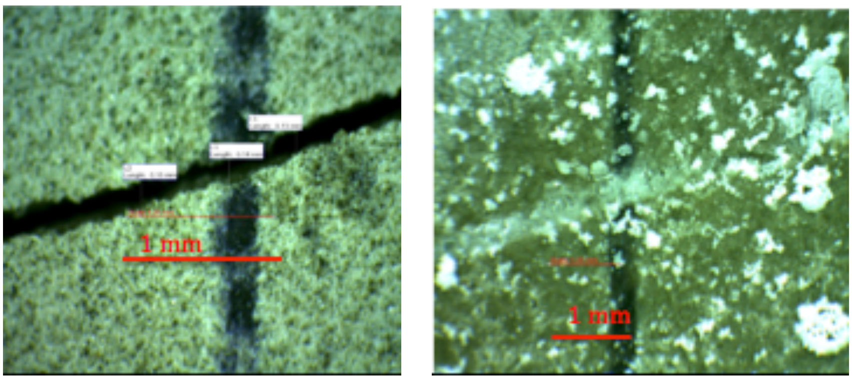

Figure 4.15- Digital Microscopy of 50:50 slag cement on Day 1 and Day 14

The following images show the typical extent of crystallisation for each mix after 14 days (figure 4.16):

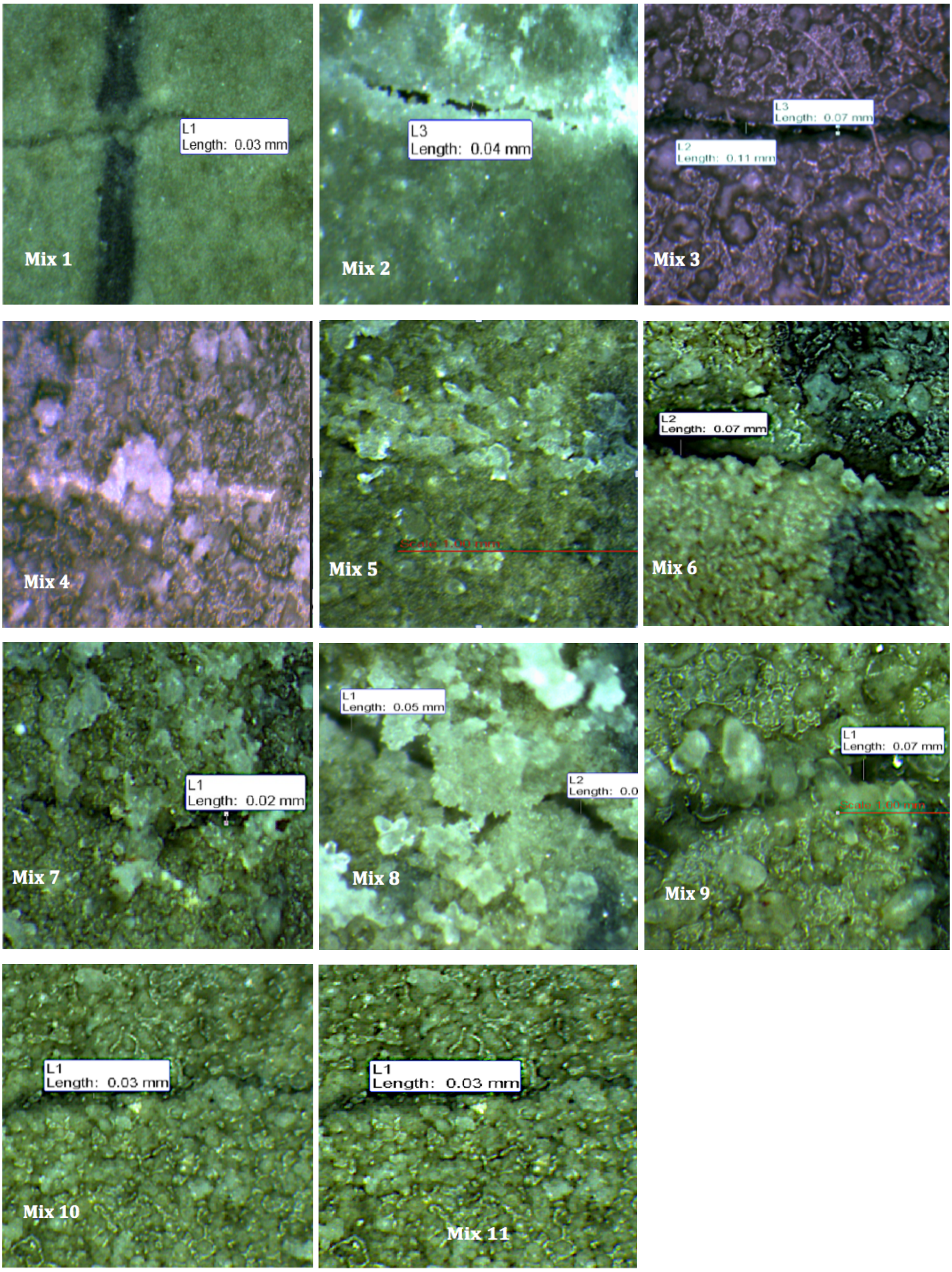

Figure 4.16- Crystallisation of Mix 1-11

4.2.2 Crack Width Measurement

The crack widths of samples were measured using digital microscopy on day 1 and day 14 after cracking the samples on day 1 using three-point bend tests. Each sample was marked in three places on one side of the prism from which an average crack width was obtained (Figure 4.17). The measurements for each of the three samples from each mix on day 1 and day 14 are shown in Table 4.2. The crack width of samples on day 1 ranged from 0.04 to 0.28mm. On day 14 this range had reduced to 0-0.11 mm. From the table it can be concluded that the addition of minerals in general has accelerated the crack healing process rate.

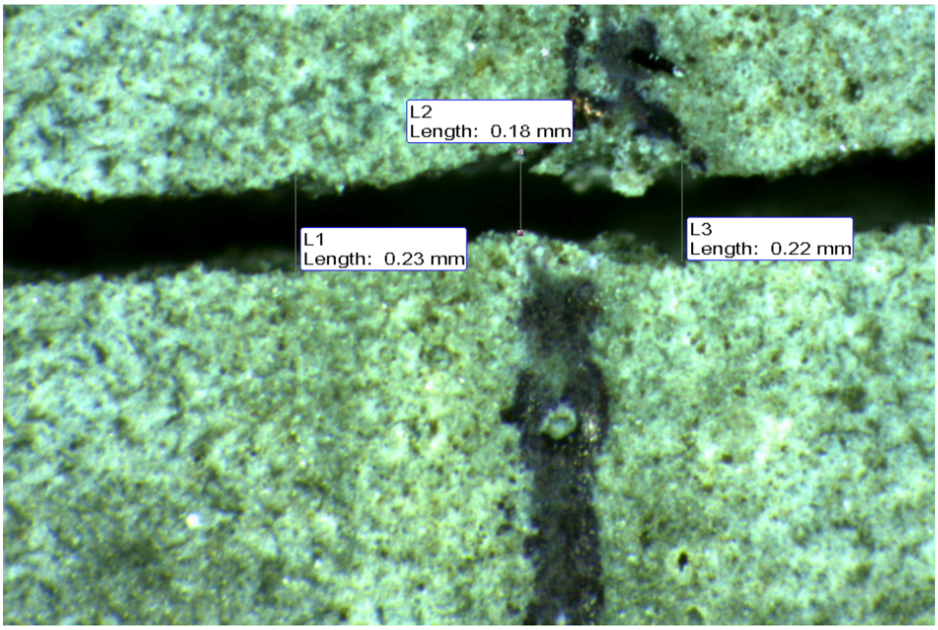

Figure 4.17-Crack Width Measurement Method

During the three-point bend test some of the samples broke completely due to brittleness, however they were put back together and the width was measured and placed upright in the curing tank to heal for 14 days. From Table 4.2 the addition of 3% and 5% MgO N50 lead to great reductions in crack width over the period of 14 days and sample 3.1 had completely healed. However most of the smallest crack widths on day 14 were observed in Mixes 6,7,10&11. In general a positive relationship could be established between the size of the crack width on day 14 and the original size of the crack width: the smaller the crack created on day 1, the smaller the crack width observed on day 14.

Mix	Sample	Day 1 Crack Width (mm)	Average Day 1 Crack Width	Day 14 Crack Width (mm)	Average Day 14 Crack Width	Average % Reduction
1	1.1	0.15	0.12±14%	0.05	0.05±17%	54.63
	1.2	0.12		0.07		
	1.3	0.09		0.04		
2	2.1	0.19	0.25±12%	0.06	0.06±16%	76.2
	2.2	0.28		0.07		
	2.3	0.27		0.04		
3	3.1	0.17	0.14±10%	0	0.06±56%	57.14
	3.2	0.12		0.06		
	3.3	0.14		0.11		
4	4.1	0.08	0.10±23%	0.06	0.05±19%	51.39
	4.2	0.08		0.03		
	4.3	0.15		0.05		
5	5.1	0.06	0.14±32%	0.02	0.06±54%	60.61
	5.2	0.22		0.1		
	5.3	0.15		---		
6	6.1	0.16	0.10±34%	0.06	0.03±40%	64.77
	6.2	0.11		0.02		
	6.3	0.04		0.02		
7	7.1	0.09	0.07±18%	---	0.02±0%	63.33
	7.2	0.05		0.02		
	7.3	0.06		0.02		
8	8.1	0.12	0.12±3%	---	0.05±0%	59.94
	8.2	0.12		0.05		
	8.3	0.13		0.05		
9	9.1	0.28	0.22±21%	0.06	0.05±16%	73.9
	9.2	0.24		---		
	9.3	0.13		0.04		
10	10.1	0.06	0.11±31%	0.03	0.04±18%	64.07
	10.2	0.18		0.05		
	10.3	0.1		0.03		
11	11.1	0.08	0.10±14%	0.03	0.03±0%	69.81
	11.2	0.1		0.03		
	11.3	0.13		0.03		

Table 4.2- Measured Crack Width of Samples on Day 1 and Day 14

4.3 Mechanical Strength

This section focuses on the analysis of the results from the three-point bend tests performed on 1-day and 14-day cured samples, as well as results from re-cracking of the 1st day cracked samples on the 14th day. The first section focuses on the strength recovery of the 1-day cured samples.

4.3.1 Mechanical Strength Recovery

Load-Displacement graphs were obtained from three-point bend tests performed on the prism samples from each mix. Figure 4.18 shows a typical load-displacement graph for mechanical strength recovery. In some cases the samples broke before performing the tests on them and therefore for those instances it was not possible to record the load-displacement data. The data was also used to produce table 4.3, showing information on the percentage recovery of mechanical strength of each of the three samples per mix to calculate an average recovery percentage for each mix. Figure 4.19 was also produced for comparison purposes based on the data obtained.

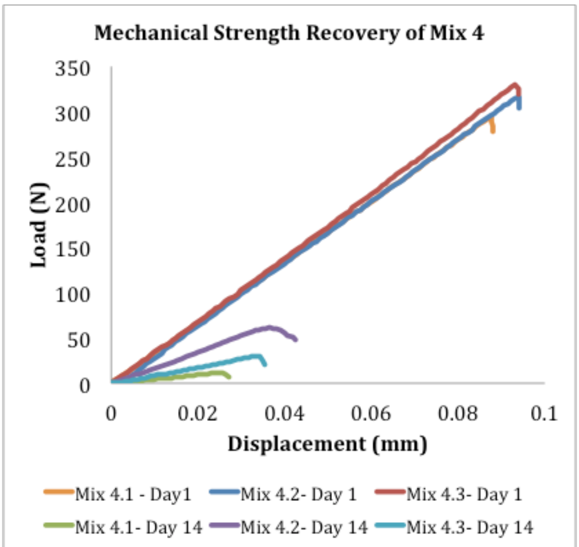

Figure 4.18- A Typical Mechanical Strength Recovery Graph

The table along with the figure go to show that in terms of average recovery percentage per mix, mixes 4-7 demonstrate the best results and that overall the addition of MgO has increased the mechanical strength recovery percentage of the mixes compared to 100% OPC or 50:50 OPC-GGBS mixes. This could also be due to the crack size of samples created on day 1, as the consistency in recovery percentage for each mix is debatable. For example for mix 6 (5% MgO 92/200), sample 3 has produced a strength recovery of 31.7% compared to 1.4 and 1.6% for samples 1 and 2 respectively. A look at table 4.7 would confirm that the large discrepancy between sample 3 and samples 1 and 2 is due to the crack size of these samples on day 1 (0.04 mm for sample 6.3 compared to 0.16 and 0.11mm for 6.1 and 2). Same trend can be recognised for mix 5. It can be concluded that controlling the crack size of samples could potentially lead to a better mechanical strength recovery as well as a better healing rate.

Another point that could be deduced from figure 4.19 is that the addition of 3-7% MgO N50 and 92/200 barely increased the mechanical strength of the samples on day 1 compared to Mix 1. In some cases it even lead to lower mechanical strengths. However, the addition of 50% GGBS to OPC significantly improved the mechanical strength of the samples in comparison to Mix 1. Addition of 3-7% MgO 92/200 to GGBS-OPC has also had a positive effect on the strength of the samples on day 1. This is in accord with the literature review, stating that the addition of GGBS results in lower early-age compressive strength, but higher flexural strength from the beginning due to increased denseness of the paste and better bonding (SCA, 2003). The samples containing GGBS yielded the lowest mechanical strength recovery percentage from all the mixes. This could be due to the low short-term hydration rate of GGBS, which leads to a higher healing rate at later stages.

Overall from figure 4.19, the addition of minerals has increased the strength recovery percentage of the samples. However, the crack size of the samples had a great role to play in determining the strength recovery of samples. This meant that samples that were broken completely on the 1st day yielded a lower strength recovery and therefore some of the results obtained from these tests were not reliable. Ideally a second set of tests should have been performed to improve the reliability of the results, however due to the imposed time limit this was not achieved.

Mix		Day 1 Peak Load (N)	Day 14 Peak Load (N)	Mechanical Strength Recovery (%)	Average Recovery (%)	% Error
1	1.1	---	---	---	1.4±0.15	±11
	1.2	408.9	6.4	1.6		
	1.3	511.9	6.4	1.3		
2	2.1	628.5	13.9	2.2	1.9±0.30	±16
	2.2	402.9	8.8	2.2		
	2.3	503.7	6.7	1.3		
3	3.1	553.3	23.4	4.2	2.0±1.15	±57
	3.2	655.6	3.5	0.5		
	3.3	683.9	7.6	1.1		
4	4.1	294.3	11.6	3.9	10.8±4.52	±42
	4.2	315.6	61.0	19.3		
	4.3	329.9	29.9	9.1		
5	5.1	486.4	74.5	15.3	9.8±5.50	±56
	5.2	479.8	20.4	4.3		
	5.3	272.7	---	---		
6	6.1	576.0	7.9	1.4	11.6±10.07	±87
	6.2	365.0	6.0	1.6		
	6.3	373.0	118.3	31.7		
7	7.1	493.3	---	---	16.9±4.10	±24
	7.2	417.0	87.5	21.0		
	7.3	457.9	58.5	12.8		
8	8.1	1409.8	---	---	1.5±0.30	±20
	8.2	1375.9	15.9	1.2		
	8.3	542.0	9.6	1.8		
9	9.1	1067.5	10.4	1.0	2.2±1.20	±55
	9.2	---	---	---		
	9.3	982.2	33.2	3.4		
10	10.1	1002.5	1.0	0.1	2.3±1.14	±50
	10.2	934.5	37.7	4.0		
	10.3	994.9	26.3	2.6		
11	11.1	947.8	9.0	0.9	1.4±0.79	±56
	11.2	856.8	25.2	2.9		
	11.3	601.8	1.6	0.3		

Table 4.3- Mechanical Strength Recovery of Samples (Cracking on Day 1 and Re-cracking on Day 14)

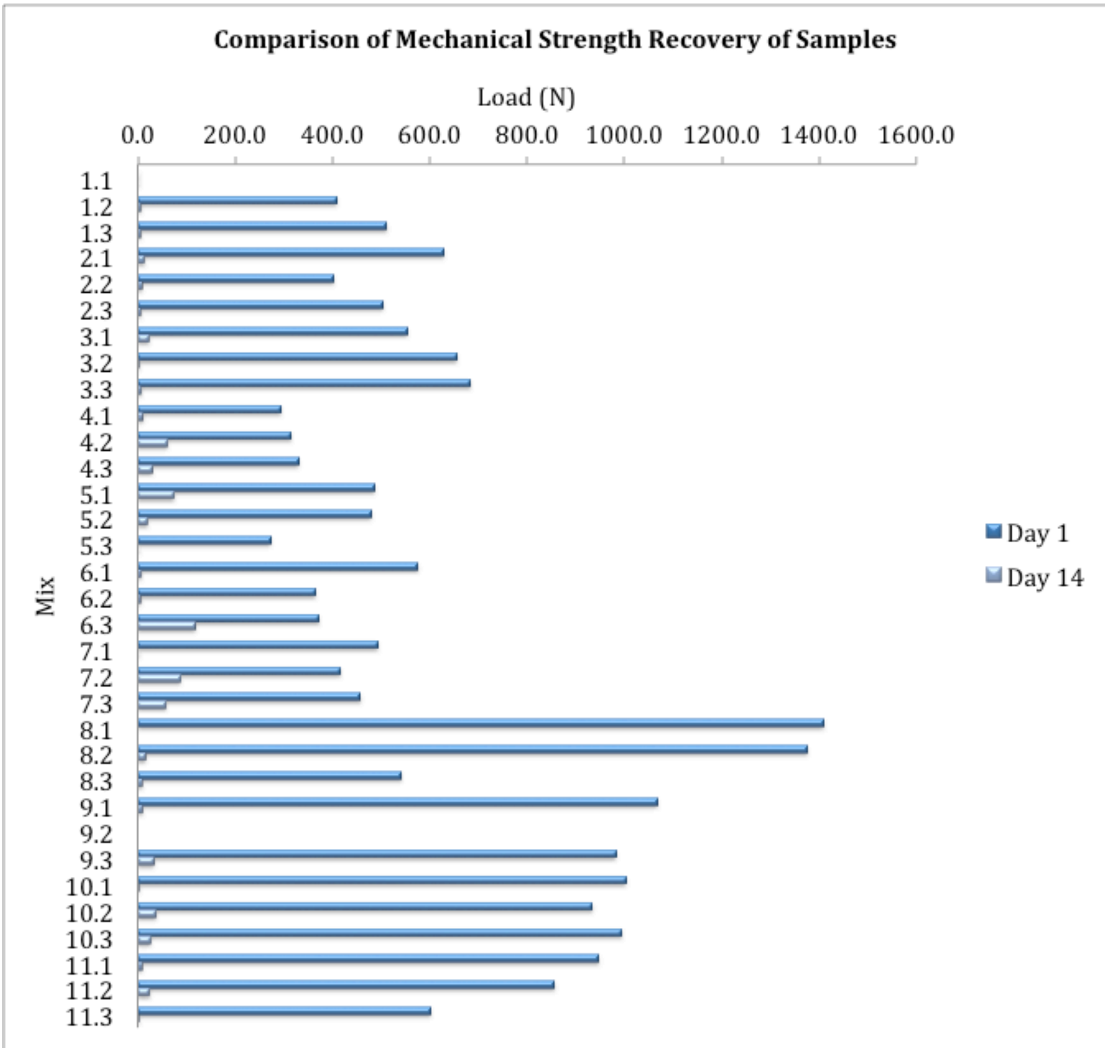

Figure 4.19-Comparison of Strength Recovery of All Mixes

4.3.2 Mechanical Strength of Day-1 Samples vs. 14-day Cured Samples

The results from the tests performed on 14-day cured samples were compared to those obtained for samples cracked on the first day of curing. Similar to the mechanical strength recovery tests, Load-Displacement graphs were obtained from the data collected. Figure 4.20 shows a typical graph. The data was also used to produce table 4.4, showing peak loads for each day from each sample to calculate the average percentage change in mechanical strength of each mix. Figure 4.21 was produced to compare the average peak load of each mix on day 1 and day 14.

Mix		Day 1 Peak Load (N)	Day 1 Average Peak Load (N)	Mix	Day 14 Peak Load (N)	Day 14 Average Peak Load (N)	% Change
1	1.1	---	460.4±11%	1.4	240	457.1±47%	-0.7
	1.2	408.9		1.5	674.2		
	1.3	511.9		1.6	---		
2	2.1	628.5	511.7±13%	2.4	948.8	982.3±3%	+92.0
	2.2	402.9		2.5	---		
	2.3	503.7		2.6	1015.7		
3	3.1	553.3	630.9±6%	3.4	1222.6	1118.9±5%	+77.3
	3.2	655.6		3.5	1010.6		
	3.3	683.9		3.6	1123.4		
4	4.1	294.3	313.3±3%	4.4	672.3	769.2±6%	+145.6
	4.2	315.6		4.5	819.7		
	4.3	329.9		4.6	815.7		
5	5.1	486.4	413.0±17%	5.4	1322.7	1193.2±6%	+188.9
	5.2	479.8		5.5	1147.9		
	5.3	272.7		5.6	1108.9		
6	6.1	576	438.0±16%	6.4	885.3	1064.2±8%	+143.0
	6.2	365		6.5	1143.7		
	6.3	373		6.6	1163.6		
7	7.1	493.3	456.1±5%	7.4	1004.3	1397.2±17%	+206.4
	7.2	417		7.5	1360.5		
	7.3	457.9		7.5	1826.9		
8	8.1	1409.8	1109.2±26%	8.4	1306.4	1142.7±14%	+3.0
	8.2	1375.9		8.5	813.5		
	8.3	542		8.6	1308.3		
9	9.1	1067.5	1024.9±4%	9.4	1611.1	1410.9±13%	+37.7
	9.2	---		9.5	1563.2		
	9.3	982.2		9.6	1058.4		
10	10.1	1002.5	977.3±2%	10.4	1850.7	1972.8±5%	+101.9
	10.2	934.5		10.5	2159.1		
	10.3	994.9		10.6	1908.7		
11	11.1	947.8	802.1±13%	11.4	--	1853.1±6%	+131.0
	11.2	856.8		11.5	1735.3		
	11.3	601.8		11.6	1970.9		

Table 4.4- Mechanical Strength of Samples Cracked on Day-1 & Day-14

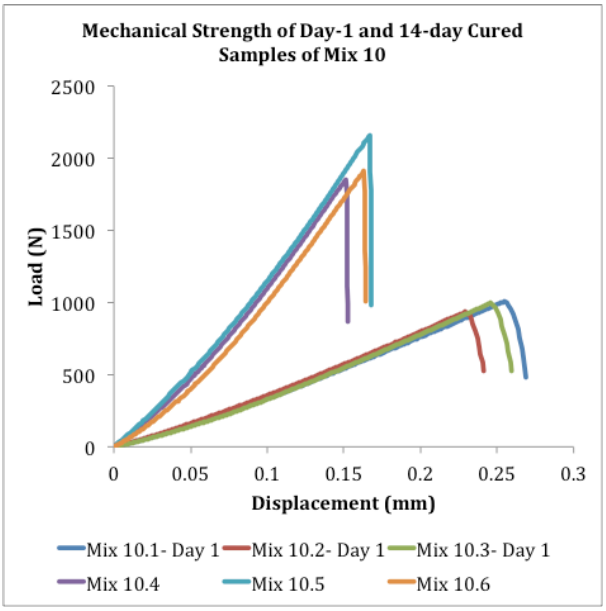

Figure 4.20- A Typical Graph of the Mechanical Strength of 1-Day and 14-Day Cured Samples

From table 4.4 and figure 4.21 it was concluded that the mechanical strength of samples significantly improved in the cases where MgO and GGBS were added to the mix (Mix 2-11). There is very little change in the average mechanical strength of 14-day cured OPC (Mix 1). Looking at sample 1.4 the peak load is much lower than that of sample 1.5. This could be random and due to a discrepancy in the composition of sample 1.4 (e.g. more brittle, inferior structural integrity). If there were more time to perform the experiments, the results for samples 1.4-6 would have been repeated to obtain a more reliable result. The general trend observed from table 4.4 and figure 4.21 is that the addition of MgO 92/200 has caused the highest increase in strength on day 14, which could be due to the delayed formation of brucite and magnesite. The addition of MgO N50 has also increased the strength, however the change in strength in comparison to day-1 samples is not as significant. The addition of 5% MgO N50 has produced the highest strength of all MgO N50 mixes on day 14. On the other hand for Mixes 5-7 the addition of 7% MgO has given the best result on day 14 and the same could be deduced for Mix 8-10, with 7% MgO addition giving the highest strength on day 14. However, Mix 11 that was a 50:50 combination of OPC and GGBS only, had yielded the second highest average strength on day 14, which could suggest that the increase in strength of Mix 8-10 could be more due to the addition of GGBS rather than MgO 92/200. Therefore the addition of 7% MgO 92/200 to the slag cement paste was expected to produce the highest strength on day 14.

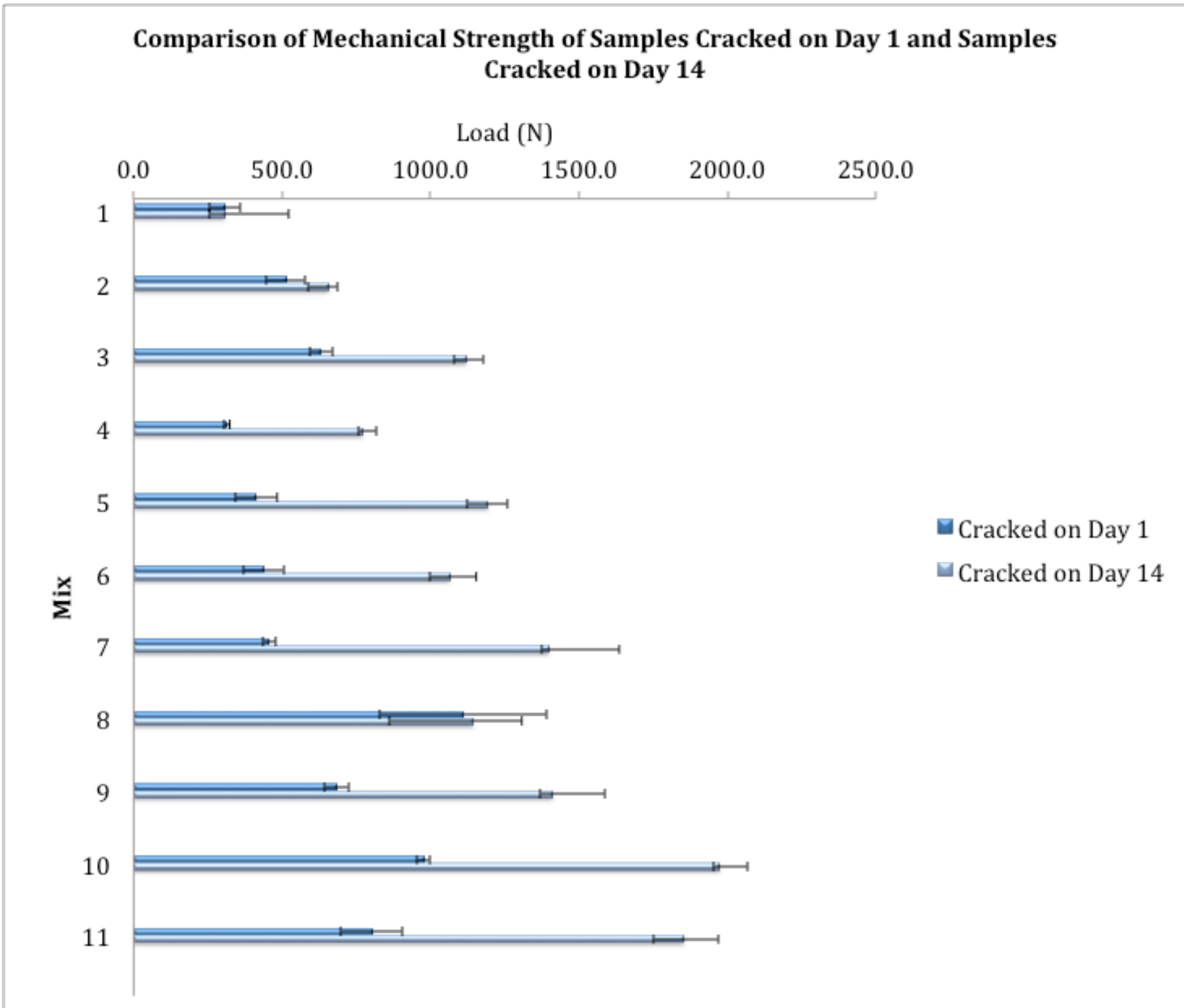

Figure 4.21-Comparison of Mechanical Strength of Mix 1-11 Cracked at Different Ages

4.4 XRD Analysis

Figure 4.22 shows the XRD pattern analysis for Mix 1,3 and 6. For Mix 1 (100% PC), the expected hydration products were observed such as ettringite, portlandite and C-S-H (cause of strength in cement) along with calcium carbonate precipitates (Calcite), which are known to be the principal products in encouraging self-healing. Taking a look at the patterns for MgO N50 and 92/200, the peaks present for MgO N50 are the same as those for 100% PC. MgO 92/200 has also produced a very similar pattern to 100% PC, with the difference that it is missing the ettringite peak. The peak at 18° for N50 and 92/200 was difficult to analyse as it could be due to the presence of both brucite and portlandite. For MgO 92/200 the peak at 43° could have been due to C-S-H and unreacted MgO, and it is difficult to say which exactly, unless the microstructure was analysed more closely using SEM or further tests. Calcite and magnesite share the same peaks on the graphs, therefore it is not possible to distinguish between the two on the graphs containing MgO. However, it has been suggested that for a large amount of magnesite to form, accelerated curing conditions are necessary (injection of CO_2). It is very unlikely for brucite to contribute by a huge amount to the peaks at 18° as with up to 7% MgO addition, it is very difficult to get a large amount of brucite formation. It would be a good idea to perform XRD tests and SEM tests to further analyse the effect of MgO addition on the mixtures and compare with the graphs already obtained.

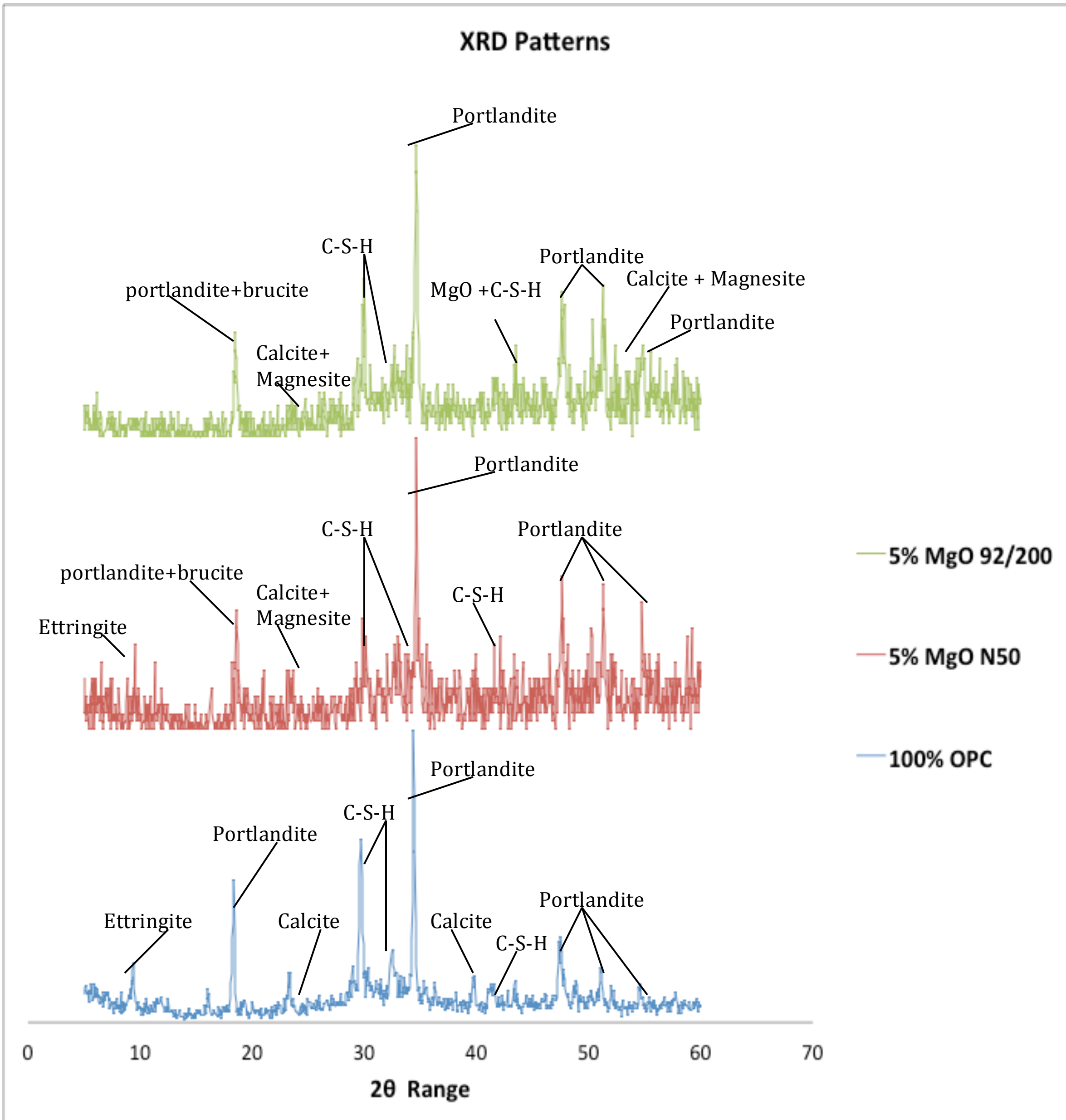

Figure 4.22- XRD Pattern Analysis for Mix 1,3 and 6

5 Conclusions

Cracks occur commonly in cementitious structures. There are various conditions that contribute to the development of cracks, the main driving force being the low tensile strength of concrete. Factors such as mechanical loading, environmental conditions and thermal shrinkage are amongst the causes of crack development (Klemczak et al., 2011). The presence of cracks is economically, environmentally and aesthetically undesirable.

Self-healing of concrete has offered a promising solution in mitigating the economical and environmental challenges faced. This report focused on the autogenic self-healing aspect, examining the effects of two types of MgO (N50 and 92/200, highly reactive and less reactive respectively) on the self-healing properties of two different cement types (Ordinary Portland cement and slag cement at an equal ratio).

MgO exhibits expansive properties upon hydration and dead-burned MgO (calcined at high temperatures) has been used in dams in China for a very long time to compensate for the long-term thermal shrinkage of concrete. However, high contents of dead-burned MgO had proven to lead to an unexpected high long-term expansion, leading to poor structural integrity. More recently, MgO fabricated at lower temperatures has been studied for improved expansive properties due to its reactive nature. It has offered advantages over other mineral additives such as higher stability and controllable properties.

The addition of ground granulated blast-furnace slag to traditional Portland cement has proven to be advantageous in terms of long-term durability, strength and environmental aspects. Addition of MgO to slag cement to investigate the effects on self-healing has not been tested on a large scale yet. Hence, in this report in addition to the effects of different types of MgO on self-healing properties of OPC, the effect of MgO on slag cement was also investigated.

Portland cement samples with up to 7% MgO content (N50 and 92/200) along with GGBS-PC blends with up to 7% MgO 92/200 were tested for compressive strength development, visible crack healing and mechanical strength recovery and development in 14 day cycles. The samples with 5% MgO 92/200 and MgO N50 along with ones made of 100% OPC were also analysed using X-Ray diffraction.

From the results and discussions it was concluded that:

(1) The addition of both types of MgO resulted in a lower compressive strength in both types of cement. The addition of 3% MgO N50 resulted in the highest compressive strength from all the N50 mixes, though it still produced a lower strength than that of 100% OPC. The addition of MgO 92/200 produced higher compressive strengths than OPC 100% on day 1, with values close to OPC on day 3, before remaining more or less constant until day 14, therefore yielding a lower compressive strength

than OPC after 14 days. This is contrary to the results obtained by TecEco Ltd., which showed that their Tec-Cement products (5-20% MgO substitution) result in higher strengths than OPC (TecEco). However the results of this report were in accordance with those from a study by Vanderperre, Liska and Al-Tabbaa (2008), in which it is stated that due to MgO content increase there is a strong decrease in strength, which could be related to the increase in porosity level of samples. Brucite is a crystalline product whereas C-S-H formed upon hydration of PC is in gel form and therefore MgO yields a more porous structure. The difference between the strength of cement pastes with MgO N50 and with MgO 92/200 could be related to the decreased hydration rate of 92/200. The addition of 5% MgO 92/200 and 3% MgO N50 resulted in the highest compressive strengths on day 14 after OPC 100%.

(2) The addition of GGBS to OPC resulted in a lower strength compared to OPC mix in the first 14 days, which was predicted from the literature review, as the activation of GGBS is dependent on the hydration of PC to form $Ca(OH)_2$. Portlandite then causes more C-S-H formation, therefore resulting in higher strengths at later stages. The addition of MgO 92/200 to GGBS-OPC mix resulted in lower strength compared to the mixes containing GGBS-OPC only. However, in contrast to the mixes containing MgO-PC only, there was an increase in strength between day 3 and 14. The addition of 7% MgO 92/200 resulted in the highest compressive strength amongst the MgO-GGBS-PC mixes, however this strength was still approximately 20 MPa lower than the highest strength for MgO-PC mixes.

(3) The autogenic self-healing of the cracks was improved with the addition of MgO. The addition of 3% MgO N50 resulted in the best crack width recovery from all MgO N50 mixes and 5% MgO 92/200 likewise resulted in the best recovery (average percentage reduction in crack width). However the general trend that was observed was that the smaller the crack width on day 1, the better the recovery of the crack on day 14. The addition of MgO 92/200 resulted in a higher crystallisation rate at the crack surfaces compared to MgO N50. This could be explained using the expansion model described by Mo et al.: The expansion of MgO 92/200 is delayed therefore there will be an increased period for its hydration which would result in more product precipitation over the course of the 14 days. Formation of brucite crystals occurs inside the pores and on the grain surface of the particles for MgO N50, therefore this could be another reason that not many precipitates are observed on the crack faces for this type of MgO. The addition of MgO 92/200 to GGBS-PC mix, did not have an improving effect on the crack recovery compared to GGBS-PC mix within the first 14 days. This could be due to the late activation of GGBS and therefore the slow recovery of samples short-term, and improved recovery and strength in long-term. For more reliable results, the tests should be performed for longer than 14 days in the future to confirm whether or not the slow recovery is only a short-term effect.

(4) The flexural strength of the samples was found to be directly proportional to the crack width created on the first day: The smaller the crack width created on day 1, the better the mechanical

strength recovery percentage of the mixes. In general it was noticed that the mixes containing GGBS yielded higher flexural strengths on day 1, with the addition of 3-7% MgO 92/200 to the mix producing samples with the highest flexural strengths (Mix 8-10). Mix 6.3 produced the highest strength after recovery on day 14 due to its small crack width on day 1. However in general it could be said that the addition of both types of MgO improved the crack healing process.

(5) When comparing the flexural strength of mixes cured for 1 day with those cured for 14 days, it was found that the addition of MgO 92/200 to the PC mixes significantly improved the flexural strength of 14-day cured samples, with a 7% content yielding the highest strength. The addition of MgO N50 also improved the flexural strength after 14 days compared to Mix 1 (100% PC), but not significantly. The same trend was observed for samples containing GGBS and PC: The addition of 7% MgO 92/200 yielded the highest strength.

(6) The hydration products of 100% PC observed were ettringite, portlandite, calcite and C-S-H. Similar peaks were observed for MgO N50 and 92/200. Brucite and portlandite share the same peaks, as do calcite and magnesite, and C-S-H and un-hydrated MgO. Therefore it was difficult to quantify the amount of hydrated products due to the presence of MgO in presence of PC and therefore it was decided that future work could include SEM, back scattering and thermogravimetric analysis to identify and quantify the presence of hydration products.

6 Risk Assessment

A full risk assessment was performed before starting the practical aspects of the project and a COSHH form was filled in for hazardous substances. The predictions on the risk assessment form had adequately covered the risks faced during testing. However, performing XRD was not included in the risk assessment performed. Hence prior to operating the XRD machine, health and safety instructions regarding the machine were received.

7 Future Work

Further work could involve:

- The use of reinforcement to limit the range of crack widths obtained on day 1, upon the performance of three-point bend tests. This could be in the shape of bars or the inclusion of fibres to prevent the formation of large cracks
- Performing XRD analyses with a better step size and on samples with different MgO contents (i.e. 3% and 7%), including the samples containing GGBS
- Performing SEM on samples to confirm the results of XRD analyses, as the results from XRD are not always reliable on their own.
- Monitoring and curing the samples for longer than 14 days, as the reactivity and healing of samples could change in the long run and it was not possible to detect that if it happened for the samples tested
- Curing of samples in a carbonated environment to analyse the effect on the healing rate and the products formed.

8 References

Ahmad,B.(2011),OPTIMIZING SELF-HEALING MECHANISM OF SLAG CEMENT CONCRETE UNDER NATURAL CARBONATION,*3rd International conference on Self-Healing Materials,*Bath.

Ahn,T.& Kishi,T. (2009),*The effect of geo-materials on the autogenous healing behavior of cracked concrete,*Taylor & Francis Group.

Antiohos,S. K.&Papageorgiou, A.(2008),Influence of quicklime addition on the mechanical properties and hydration degree of blended cements containing different fly ashes,*Construction and Building Materials,22*,1191-1200.

Barca,I. K.(2007, January),*Effects of Ground Granulated Blast Furnace Slag in Portland Cement Concrete- Expanded Study,*Retrieved 01 2014 from Wisconsim Highway Research Program:http://wisdotresearch.wi.gov/wp-content/uploads/05-01slagexpanded-fr1.pdf

Barron,A. R.(2010, January 26),*Hydration of Portland Cement,*Retrieved 03 04,2014 from Openstax: http://cnx.org/content/m16447/latest/

CSI.(n.d.),*Cement Production,*Retrieved 03 2014 from World Business Council for Sustainable Development:Cement Sustainability Initiative: http://www.wbcsdcement.org/index.php/about-cement/cement-production

Dry, C. M. (1992),Smart Building Materials which Prevent Damage or Repair Themselves,*MRS proceedings, 276, 311 doi: 10.1557/PROC-276-311.*

Edvardsen,C.(1999),*Water Permeability and Autogenous Healing of Cracks in Concrete,*ACI Materials Journal.

European Commission,(2010, May),*Cement, Lime and Magnesium Oxide Manufacturing Industries,*Retrieved 05 2014 from http://www.umweltbundesamt.de/sites/default/files/medien/419/dokumente/clm_bref_0510.pdf

Gao,P.& Lu,X.(2008),Production of MgO-type expansive agent in dam concrete by use of industrial by-products,*Building and Environment,43*(4),453-457.

Ghosh,S.K.(2009),*Self-healing Materials: Fundamentals,Design Strategies,and Applications.*Wiley-VCH.

Global CCS Institute. (2013, 02 20). *An update on CO2 capture from cement production*. Retrieved 02 01, 2014 from http://www.globalccsinstitute.com/insights/authors/dennisvanpuyvelde/2013/02/20/update-co2-capture-cement-production

Heriot-Watt University,(2012),*Condition Monitoring System for Reinforced Concrete Structures,*Retrieved April 2014 from www.hw.ac.uk/documents/Condition-Monitoring.pdf

Hosoda,A.& Kishi,T.(2007),SELF HEALING OF CRACK AND WATER PERMEABILITY OF EXPANSIVE CONCRETE. *The First International Conference on Self Healing Materials*(pp. 1-10),Noordwijk aan Zee:Springer.

IEA,(2009, December),*Technology Roadmap:Cement*,Retrieved 01 25, 2014 from http://www.iea.org/publications/freepublications/publication/name,3861,en.html

Jin,F.&Al-Tabbaa,A.(2014),Strength and hydration products of reactive MgO–silica pastes,*Cement and Concrete Composites,52*, 27-33.

Klemczak,B.& Knoppik-Wrobel,A.(2011),EARLY AGE THERMAL AND SHRINKAGE CRACKS IN CONCRETE STRUCTURES–DESCRIPTION OF THE PROBLEM,*Architecture Civil Engineering Environment,2*,35-48.

Li,F.-X,(2010),INFLUENCE OF MgO EXPANSIVE AGENT ON BEHAVIOR OF CEMENT PASTES AND CONCRETE,*The Arabian Journal for Science and Engineering,35* (1B),125-139.

Mehta,P,(1978),*Cement Standards:Evolution and Trends.*Baltimore, USA:American Society for Testing and Materials.
Mehta,P. K.&Pirtz, D.(1980),Magnesium Oxide Additive for Producing Self-stress in Mass Concrete,*The 7th International Congress on the Chemistry of Cement,3*,pp.6-9,Paris.

Mo,L.,Deng,M.&Al-Tabbaa,A.(2014),MgO expansive cement and concrete in China:Past, present and future,*Cement and Concrete Research,57*,1-12.

Mo,L.,Deng,M.&Tang,M.(2010),Effects of calcination condition on expansion property of MgO-type expansive agent used in cement-based materials,*Cement and Concrete Research*,*40*(3),437-446.

Mortar Industry Association(2012, May),T*he use of ground granulated blastfurnace slag and fly ash in mortar.*Retrieved 02 2014 from http://www.mortar.org.uk/documents/miadata16-mono.pdf

Nagataki,S.&Gomi,H.(1998),Expansive admixtures,*Cement and Concrete Research,21*(11),163-170.

Neville,A.M.(1994),*Properties of Concrete,*Great Britain:Longman Scientific & Technical.

Nishiwaki,T.,Jang,B.-K.&Mihashi,H.(2006),Development of Self-Healing System for Concrete with Selective Heating around Crack.*Journal of Advanced Concrete Technology,4*(2),267-275.

Odler,I.&Colán-Subauste,J.(1999),Investigations on cement expansion associated with ettryngite formation.*Cement and Concrete Research,29*,731-735.

Oner,A.&Akyuz,S.(2007),An experimental study on optimum usage of GGBS for the compressive strength of concrete. *Cement and Concrete Composites,29*(6),505-514.

Ramm&Biscoping(1998),Autogenous healing and reinforcement corrosion of water-penetrated separation cracks in reinforced concrete,*Nuclear Engineering and Design,179*(2),191-200.

Regourd,M.(1980),Structure and Behavior of Slag Portland Cement Hydrates.*Seventh International Congress on the Chemistry of Cement,1*,pp. 63-67.

Reinhardt,H.-W.&Joos,M.(2003).Permeability and self-healing of cracked concrete as a function of temperature and crack width.*Cement and Concrete Research,33*(7),981-985.

RILEM(2013),*Self-healing phenomena in cement-based materials.*RILEM.

Scientific American(2008, August).*Cement from CO2:A Concrete Cure for Global Warming?*Retrieved 03 2014 from Scientific American: http://www.scientificamerican.com/article/cement-from-carbon-dioxide/

Shand,M. A.(2006).*The Chemistry and Technology of Magnesia.*New Jersey,USA:John Wiley & Sons.

Shi,C.(2001),STUDIES ON SEVERAL FACTORS AFFECTING HYDRATION AND PROPERTIES OF LIME-POZZOLAN CEMENTS,*Materials in Civil Engineering ,13*,441-445.

Siddique,R.&Bennacer,R.(2012),Use of iron and steel industry by-product(GGBS) in cement paste and mortar. *Resources,Conservation and Recycling,69*,29-34.

Slag Cement Association(2003),*Compressive and Flexural Strength,* Retrieved April 2014 from http://www.slagcement.org/News/pdf/No14_Compress_Strength.pdf

Targan,S.,Olgun,A.&Erdogan,Y.(2002),Effects of supplementary cementing materials on the properties of cement and concrete.*Cement and Concrete Research,32*(10),1551-1558.

TecEco.(n.d.).*TecEco Cements*.Retrieved April 2014 from TecEco Ltd.: http://www.tececo.com/technical.tececo_cements.php

Telesca,A.,Marroccoli,M.&Pace,M. L.(2013),Expansive and non-expansive calcium sulfoaluminate-based cements.*Third International Conference on Sustainable Construction Materials and Technologies.*

Ter Heide,N.(2007),SELFHEALING OF EARLY AGE CRACKS IN CONCRETE,*Proceedings of the First International Conference on Self Healing Materials.* Noordwijk aan Zee: Springer.

Tittelboom,K. V.,Gruyaert,E.&Rahier,H.(2012),Influence of mix composition on the extent of autogenous crack healing by continued hydration or calcium carbonate formation,*Construction and Building Materials*,*37*, 349-359.

Unluer,C.& Al-Tabbaa, A.(2013).Impact of hydrated magnesium carbonate additives on the carbonation of reactive MgO cements. *Cement and Concrete Research,54*,87-97.

USGS(2012, January 24),*Mineral Commodity Summaries 2012*.Retrieved February 2,2014 from http://minerals.usgs.gov/minerals/pubs/mcs/2012/mcs2012.pdf

Van Oss,H.G.(2002).Cement Manufacture and the Environment.*Industrial Ecology,6*(1),89-105.

Vandeperre,L.,Liska,M.&Al-Tabbaa,A.(2008).Hydration and Mechanical Properties of Magnesia,Pulverized Fuel Ash, and Portland Cement Blends.*Journal of Materials in Civil Engineering,20*(5),375-383.

Vision2020(2006, June 16).*A Vision for the Concrete Repair,Protection and Strengthening Industry.*Retrieved 03 04, 2014 from http://www.concretesdc.org/_pdfs/Vision2020-Version1.0_%20May2006.pdf

Yang,Z.X.,Hollar,J.,He,X.D.&Shi,X. M.(2011).A self-healing cementitious composite using oil core/silica gel shell microcapsules.*Cem. Concr. Compos,33*,506-512.